The Extended Branch-Arrow Model (XBAM) of the Formation of Retino-Tectal Connections

Kenneth J. Overton & Michael A. Arbib

COINS Technical Report 81-14

(June 1981)

This work was supported by the National Institute of Health under grant number R01 NS14971-03.

Abstract

This paper presents XBAM (the Extended Branch-Arrow Model), a new model of the development of the retino-tectal topographic mapping as observed in frog, toad, and goldfish visual systems. The updating process employed by XBAM is distributed in nature and depends upon interactions between branches of retinal fibres, the branches and the boundaries of the tectum and of grafts, and the branches and the tectal surface. Results of computer simulation of the model are related to experimental data obtained from tectal and retinal graft and lesion studies and comparisons are also made with other models.

I. Introduction

Many experiments study the development of the topographic mapping between the retina and tectum of various lower vertebrates. Goldfish, frog, and toad visual systems have generally been the targets of these studies. In these animals the fibres from each retina project to the contralateral tectum. Early behavioral studies (Sperry 1943, 1944, 1945) (Maturana et al., 1959) showed that the visual fields of these animals would regrow to map in an orderly way after surgical interruption. With the development of electrophysiological recording techniques, investigators have been able to better understand the details of the mapping (Gaze et al. 1963, 1965, 1970, 1974) (Jacobson 1965) Stimuli in the superior section of the visual field project to the medial section of the contralateral tectum while those in the inferior field project to the lateral side. Similarly, stimuli in the nasal portion of the visual field project to the rostral end and temporal stimuli to the caudal end of the contralateral tectum (see Figure I.1). As the body of experimental data has grown, numerous models of the process by which the mapping is formed have been proposed. The models can be divided into two general classes: those subscribing to the idea of a point-to-point chemoaffinity between the retinal and tectal cells and those using the idea of systems matching.

Figure I.1

Sperry (Sperry 1944, 1945, 1963) first proposed the idea of chemoaffinity between the layers of cells. Under this hypothesis, each retinal cell is uniquely labeled according to its position on the retina. The tectal surface is considered to be labeled in a similar manner and organization of the map is the result of each retinal cell axon seeking the point on the tectum which matches its own retinal label. The Marker Induction model of Willshaw and von der Malsburg (Willshaw 1979) may be viewed as a sophisticated development of this idea in that the tectal "addresses" are not prespecified, but rather develop as a result of the interactions between the tectum and retinal fibres.

In system matching models (Gaze 1972), the information available to the retinal fibres is considerably less specific. Retinal fibres do not seek a particular point on the tectum, but rather seek a neighbourhood where the interactions with the surrounding fibres match the activity on the retina. The Arrow Model proposed by Hope et al. (1976) may be placed in this class.

While the Marker Induction and Arrow models employ different underlying assumptions as to the amount and type of information required by the organization process, they both explain many aspects of the experimental data. The model presented in this paper combines new ideas with concepts from both of these approaches to produce a hybrid model which explains a wide body of experiments.

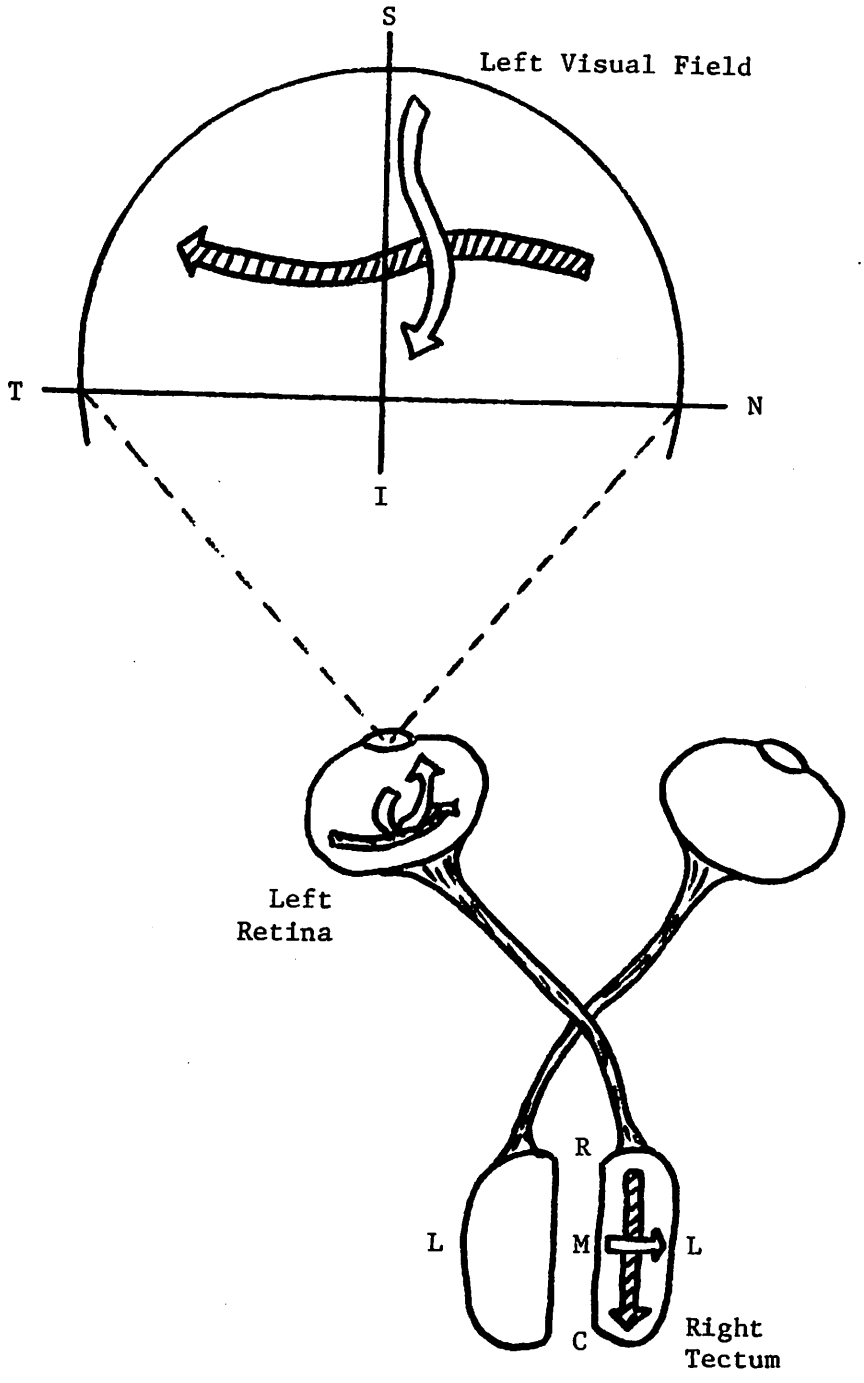

Figure I.1 Schematic of the frog visual system. Fibres from the retina project onto the contralateral tectum. Tectum: R - Rostral, C - Caudal, M - Medial, L - Lateral. Visual Field: N - Nasal, T - Temporal, S - Superior, I - Inferior.

II. System Matching

In this section, we discuss the system matching idea as represented by the Arrow Model in more detail. The Arrow Model of Hope, Hammond, and Gaze (1976), uses the relative spatial positions of the points of origin of the retinal fibres and their relative termination positions on the tectum to determine the "sorting out" of retinal fibres at the tectal surface. The use of this information in a distributed, iterative process is sufficient to account for a majority of the physiological data without recourse to any "absolute addressing" of the tectum in terms of retinal coordinates.

In the Arrow Model, the tectum is modelled as a discrete grid with retinal fibres allowed to terminate only at the intersections of the grid lines, called tectal sites. Each iteration of the sorting process may assume one of the two forms: switching interaction or random walking.

One iteration of switching interaction applies the following interchange rule to each retinal fibre, T_k. One of the eight sites immediately adjacent to the present tectal site of T_k (see Figure II.1a) is chosen at random until one containing another fibre, T_n, is found. It should be noted that the boundaries of the tectum are only implicitly considered in that a termination site on a boundary has only five neighbours. The retinal locations, R_k and R_n, of the somas from which fibres T_k and T_n, respectively, emanate are compared and the following process is used to determine the new grid location of the termination of the fibres, (Figure II.1.b).

Figure II.1a,b

* Construct a line, L_t, on the tectum which passes through the site of termination of fibre T_k and is orthogonal to the line connecting the termination sites of both fibres, T_k and T_n.

* Construct a line, L_r, on the retina which passes through the retinal position, R_k, of the soma of fibre T_k and is orthogonal to the line passing through the retinal locations of both fibres, R_k and R_n (Figure II.1.b).

* With the superior-inferior retinal axis mapped onto the medial-lateral tectal axis and the nasal-temporal retinal axis mapped onto the rostral-caudal tectal axis, switching is determined as follows: if T_n resides on the same side of line L_t as R_n does with respect to line L_r, then T_k and T_n retain their original locations, otherwise they switch positions.

This process is applied to all fibres in such a way that no fibre interacts with more than one other fibre during any iteration. Repeated application of this process produces an ordered mapping from one in which the initial positions were randomly assigned.

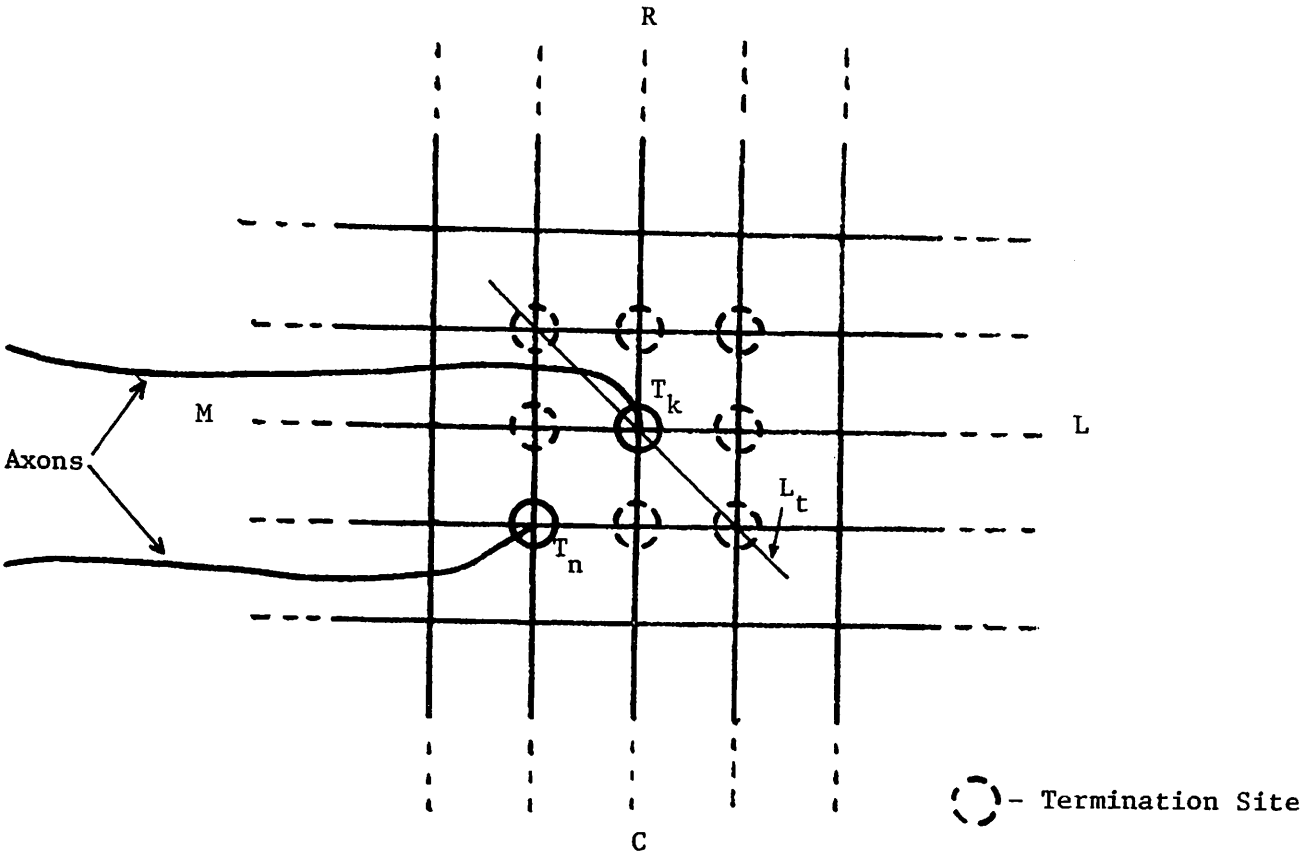

II.1a

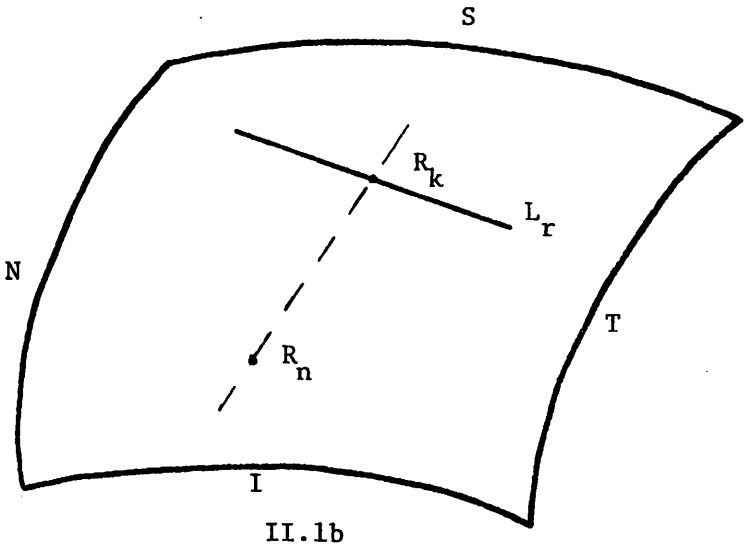

II.1b

Figure II.1 a) The grid configuration used in the Arrow Model. b) Retinal locations R and R of the somas of fibres terminating at tectal sites T and T . R - Rostral, C - Caudal, M - Medial, L - Lateral, N - Nasal, T - Temporal, S - Superior, I - Inferior.

Using this mechanism alone, there is no way for fibres to move into previously unoccupied termination sites, an ability required to explain the expansion data for a hemiretina projecting onto a complete tectum (see Section IV). In order to circumvent this problem, the fibres are periodically allowed to take random steps. During an iteration of random walking, a site adjacent to each fibre is chosen at random. If the site is empty, the fibre moves to occupy that location. If the site is occupied or, one or more other fibres are trying to move into it, the fibre retains its original location. One iteration of random walking consists of applying this process to each fibre on the tectum. The updated positions form the initial state for the succeeding iteration.

The overal sorting method involves the use of switching interaction and random walking. The majority of the iterations will employ the switching interaction while a few, spaced at predetermined intervals, will employ the random walk. The use of the random walk allows the fibres to disperse to all parts of the tectum while the switching interaction provides a degree of ordering in the mapping.

III. The Branch-Arrow Model

Our Branch-Arrow Model (BAM) redefines the Arrow Model in several ways. Recall that in the Arrow Model, retinal fibres must terminate at discrete points on a grid. In BAM, retinal fibres form several branches as they reach the tectal surface which is now modelled as a continuum rather than a grid. The termination of each branch is surrounded by a circle which represents the area of interaction with other branches (see Figure III.1). Further, each branch explicitly interacts with the tectal and graft boundaries. These changes also dictate that the neighbourhood interaction rules be modified. In our model the neighbourhood interaction process is applied to each branch so that the actual position of a fibre as a whole is determined implicitly by the locations of its branches. The resultant model, BAM, seems to more closely resemble the physiology of fibre movement. However, there is a small number of experiments which cannot be accounted for by either the Arrow Model or BAM. The Extended Branch-Arrow Model, XBAM, adds fibre-surface interaction to the Branch-Arrow Model. This extended version appears to account for an even larger body of experimental data and will be discussed in Section VIII.

Figure III.1

The BAM updating process is obtained by averaging three components: the interaction influence, $\vec{I}_b$, the boundary effect, $\vec{E}_b$, and the average influence, $\vec{A}_b$. The interaction influence component, $\vec{I}_b$, is a continuous analogue of the Arrow-Model interaction process, employed at the level of the branches of a fibre combined with a term describing the local interactions between the branches and the boundaries of the tectum and the various grafts. The average of the physical influence, $\vec{A}_b$, felt by all of the branches of a given fibre is calculated. The ultimate movement of a particular branch is then determined as the weighted sum of these influences.

$$\vec{M}_b = a_1\vec{I}_b + a_2\vec{E}_b + a_3\vec{A}_b \qquad (1)$$

where a_1, a_2, and a_3 are weighting constants, $\vec{I}_b$ and $\vec{E}_b$ are described in equations (3) and (4) below, and the average influence is given by

$$\vec{A}_b = \frac{1}{m} \sum_{k \in F_b} (a_4\vec{I}_k + a_5\vec{E}_k) \qquad (2)$$

where the sumation ranges over the set F_b of all branches k from the same retinal fibre as b, m is the number of branches in F_b, and a_4, a_5 are weighting constants.

The first term in the physical influence component provides the extension of the Arrow Model. In the Arrow Model, only one of a fibre's eight immediate neighbours is involved during each iteration of its updating. As a result, the fibre in question receives no influence from any of the other neighbouring fibres, nor from any of the fibres which do not occupy immediately adjacent sites. In BAM, the continuous nature of

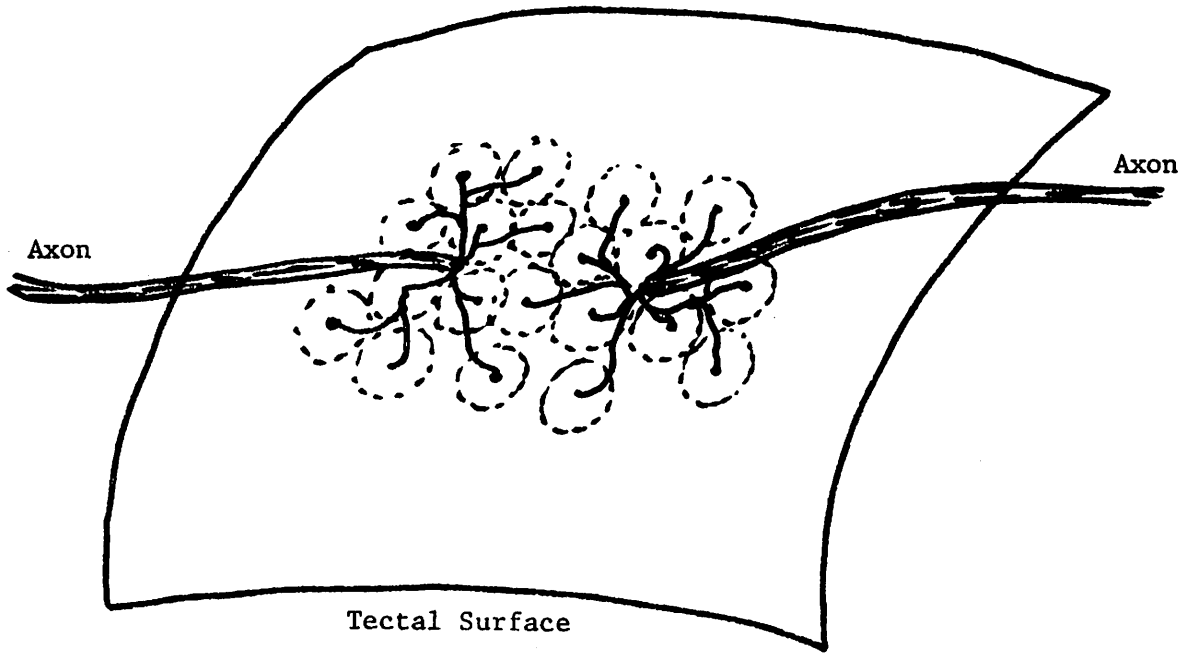

Figure III.1 Axonal arborization: retinal fibre termination configuration used in BAM and XBAM.

the tectal surface, the fact that each fibre has a set of branches, and the circle of interaction for each branch eliminate these restrictions. Due to the continuous nature of the tectal surface, the updating process is truly a neighbourhood interaction rather than an interchange. During each iteration, a branch interacts with all other branches whose circles of interaction have a non-empty intersection with the circle of the branch in question. to produce the interaction component, $\vec{I}_b$.

To see the shape of this interaction, let B_b be the set of fibre-branches whose interaction circles intersect that of branch b. Let $\vec{U}(b,k)$ be the unit vector in the "interchange direction" for the current position of b and that of k. Then the movement of b induced by its interaction with k is

$$W_d(b,k)\ W_g(b,k)\ \vec{U}(b,k)$$

where the weights W_d (due to the distance of separation) and W_g (due to interaction across a boundary) are described below in equations (4) and (5). Thus the total interaction component is given by

$$\vec{I}_b = \sum_{k \in B_b} W_d(b,k)\ W_g(b,k)\ \vec{U}(b,k) \qquad (3)$$

The direction determination, $\vec{U}_b$, is very similar to the interchange rule used in the Arrow Model. The main difference lies in the fact that if the somas are separated by a distance greater than a specified value, the direction of the influence is chosen at random. We feel that retinal cells may communicate in a meaningful way only if their somas are within a certain distance, e.g. if their receptive fields overlap. Thus if the cells are separated by a great distance, no communication is possible. When the soma of two interacting branches are within the distance allowing meaningful communication, the direction is chosen as in the Arrow Model. If the branch terminations are oriented on the tectum the same relative to some axis system as are the somas on the retina relative to the corresponding axis system, the influence tends to force the branches apart. If, however, the branch positions are reversed compared to the relative soma locations of the retina, the influence tends to force the branches to move past one another, i.e. interchange positions. In the case where both of the interacting branches in question belong to the same fibre, the influence felt by one from the other always tends to force the branches apart thereby attempting the maximize the area of the tectum covered by a fibre. The second component of the physical influence involves the interaction between the branches and the tectal and graft boundaries.

In the Arrow Model, the interchange of two fibres occurs in discrete steps. When it has been determined that two branches are oriented in the reverse of their retinal locations, they simply exchange positions. In BAM, the influence between two branches, W_d, is graduated depending upon separation. The weight is linear in nature with a value of 1 when the two branches terminate at the same point and 0 when the branches are separated by a distance of twice the radius of their circles of interaction:

$$W_d(b,k) = \begin{cases} 1 - \frac{d(b,k)}{2r} & \text{if } d(b,k) < 2r \\ 0 & \text{otherwise} \end{cases} \qquad (4)$$

where r is the radius of interaction on the tectum and d(b,k) denotes the distance between the tectal terminations of fibres b and k.

The weight due to intervening graft boundaries, W_g, is intended to model the discontinuous nature of such edges. Since the edges of grafts are actual surgical disruptions of the surface, wee feel that communication across a graft edge should be attenuated. This is expressed mathematically by including a mulplicative constant for each boundary between the two branches, so that two branches separated by a boundary exhibit less influence on one another than do two branches separated by a similar distance but with no intervening boundaries.

$$W_g(b,k) = a_g^n \qquad (5)$$

where a_g is the mulplicative constant determining cross-boundary communication effectiveness, $0 \leq a_g \leq 1$ and n is the number of graft boundaries intersecting the line segment connecting the terminations of branches b and k.

The simple Arrow Model does not include the boundary of the tectum nor the edges of the grafts as influencing factors. The second term of equation (1) includes this factor explicitly as $\vec{E}_b$.

$$\vec{E}_b = \sum_{q \in Q} W_d(b,q)\ W_g(b,q)\ \vec{U}(b,q) \qquad (6)$$

where Q is the index set of all tectal and graft boundaries; $\vec{U}(b,q)$ is the unit vector along the line perpendicular to boundary q and passing through the termination of branch b; W_d is the weight due to the distance of separation; and W_g is the weight due to graft boundaries.

Tectal and graft edges are physical discontinuities in the surface of the tectum. It should, therefore, be more difficult for an axon to migrate across such a boundary than to move across an unobstructed surface. The boundaries thus have influence by restricting the movements of the branches. As in the case of interacting branches, the magnitude of the influence, W_d, is proportional to the distance from the center of the branch circle to the boundary along a line perpendicular to the boundary.

$$W_d(b,q) = \begin{cases} 1 - \frac{d(b,q)}{r} & \text{if } d(b,q) < r \\ 0 & \text{otherwise} \end{cases} \qquad (7)$$

where r is the radius of interaction on the tectum and d(b,q) denotes the distance between the termination of branch b on the tectum and boundary q. In addition, due to the physically discontinuous nature of a boundary, the influence of one branch on another across a boundary is decreased, via W_g. Mathematically, the influence due to boundary interaction felt by branch k is given in (5). The direction of the influence, $\vec{U}$, is always away from the boundary along a line perpendicular to the boundary through the point of termination of the branch in question.

The actual influence, $\vec{M}_b$, used to update the position of a branch b during an iteration is determined as the weighted sum of the physical influences $\vec{I}_b$ and $\vec{E}_b$ felt by the branch and the average $\vec{A}_b$ of the physical influences of the branches from the same fibre, as we saw in equation (1). Since, by definition, the branches of a fibre are connected to one another, we feel that this form of information transfer can take place.

The Branch-Arrow Model incorporates the above defined neighbourhood and boundary interaction mechanisms to produce behavior accounting for essentially all of the experimental data. However, this model cannot account for the translocation experiment results since the branches are supplied with only directional information. The Extended Branch-Arrow Model builds upon the Branch-Arrow Model by the addition of global information. This will be incorporated, in Section VIII, as the fourth factor in the physical influence component which describes the interaction of the branches and the tectal surface.

IV. Experimental data compared to simulation behavior for BAM

This section presents some of the typical experimental results obtained during electrophysiological recording after various tectal and retinal lesioning. The experiments performed to date have include studies of the mapping after complete and partial ablations of the tectum as well as studies of mappings to tecta which have had sections surgically excised, rotated, inverted, or translocated and then reimplanted. Experiments involving hemiretina and compound eyes have also been performed as have studies of the initial development of the retinotectal projection. The following is a discussion of the simulation behavior of the BAM in light of these physiological experiments. Results of computer simulation of the BAM are compared with the results of the experiements. The results presented below were obtained through computer simulation of a one-dimensional retina/tectum pair containing 40 fibres, each with 4 branches. A one-dimensional simulation was utilized to reduce the amount of computation required. A sample set of simulations of two-dimensional arrangements have been performed and the results yield behavior as expected.

Experiment I.

Visual fields of lower vertebrates such as frogs and goldfish map in an ordered and predictable way onto the tectum (Yoon 1973) (Gaze 1974). In the simplest of the physiological experiments, the optic nerve is severed and both the retina and tectum are left intact. Figure IV.1 illustrates the typical findings from a normal animal with an intact retina projecting to a normal tectum. Once the tectum has been reinnervated, the mapping between the visual field and the tectal surface is studied. The data are typically obtained by electrophysiologically recording from a point on the tectum while presenting the animal with controlled visual stimuli. The location of the stimulus eliciting the greatest response from the area being recorded is said to indicate the point of emanation on the retina of the fibres being recorded.

Figure IV.1

The simulation results appear in Figure IV.2. The one-dimensional tectal surface is represented along the horizontal axis of the display. Similarly, the visual field appears along the vertical axis. Each horizontal row of symbols represents one fibre with each symbol in the row marking the position of the termination of an individual branch of the fibre. Thus for each branch of each fibre, the position in the visual field of the stimulus exciting the fibre, and thus the retinal location of the branch's soma is indicated by the height of the row on which the symbol appears. The position of the branch on the tectum is indicated by the horizontal position along the row. Further, the lower end of the visual field display maps to the leftmost end of the tectum and the upper end of the visual field display maps to the rightmost end of the tectal representation. Thus a normal mapping is depicted by a diagonal line of

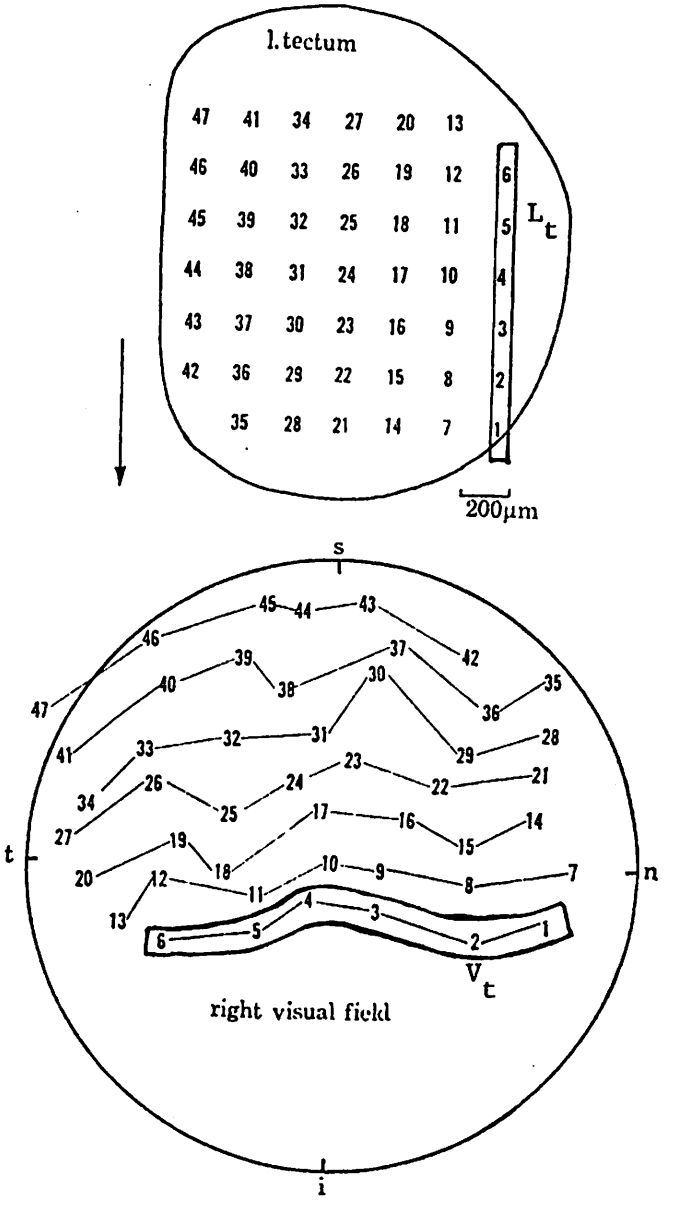

Figure IV.1 The projection of right visual field onto the left tectum in a normal animal (Gaze 1974). Lt: a single line of electrode positions which is analogous to the one-diemnsional tectum in BAM and XBAM. Vt: the corresponding single row of points in the visual field which excite the tectal positions - analogous to the vertical axis of the BAM/XBAM display.

symbols from the lower left corner of the display to the upper right.

The physiological data are inherently two dimensional. To compare the simulation results with these data, equate the vertical axis of the simulation display with the striped bar, A, in the lower half of Figure IV.1 and the horizontal axis with bar B in the upper half. The left end of the tectal representation corresponds to the lower, rostral, end of the bar in the upper half of the figure while the lower end of the retinal representation corresponds to the right, nasal, end of the bar in the lower half of the figure.

Figure IV.2

Figure IV.2.a shows the initial configuration of the fibres and branches. The branches are randomly distributed across the tectal surface. Figures IV.2b, c, d, and e depict the simulation results after 2000, 4000, 6000, and 8000 iterations of the Branch-Arrow Model as defined in the previous section. Global organization is apparent at iteration 8000 as indicated by the diagonal nature of the display. During the course of the simulation, another interesting feature is apparent. If the size of the projection field of a fibre is determined by the extent of its branches, one sees that the projection field is initially quite large. As the mapping organizes, the branches of each fibre tend to move together resulting in progressively smaller projection fields. Similar results have recently been observed by Humphery and Beazley (1981) in the frog visual system after optic nerve section. For this simulation, the radius of effective communication among the somas on the retina was set such that all cells, regardless of their separation, could exchange information. The effect of varying this parameter is the subject of the next experiment. This situation most closely resembles the Arrow Model. The weighting constants a_1, a_2, a_3, $a_4$and $a_5$in equations 1 and 2 were assigned the values of 0.25, 0.25, 0.5, 0.35, and 0.65 respectively.

These simulation results demonstrate that at least in the simplest case, the Branch-Arrow Model can produce an ordered mapping.

Experiment II.

The purpose of this experiment was to study the effects of varying the maximum distance allowing effective communication between cells on the retina. The initial state and weighting constants remained as in Experiment I. Figure IV.3a shows the organization resulting after 8000 iterations with the radius set to allow effective communication over roughly two thirds of the retina. That is, if two cells are separated by a distance greater than two thirds of the total retinal expanse, then they cannot meaningfully communicate. Thus branches at opposite ends of the retina interact at random. The resulting configuration shows two organized maps on the tectum. The simulation results depicted in Figure IV.3b show the state after 8000 iterations with the radius set to roughly one half of the total retinal size. In this case, three maps are produced. Figure

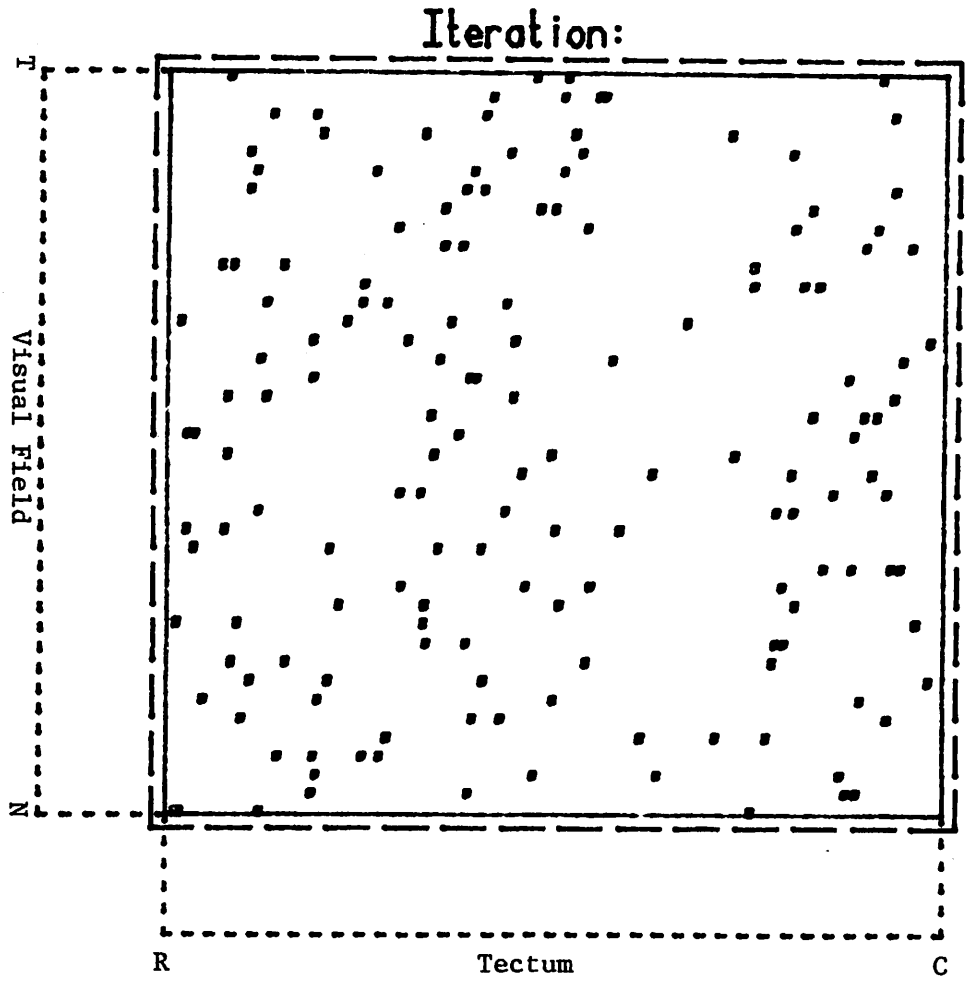

Figure IV.2a The initial distribution of branch terminations for the BAM simulation. 40 Fibres with 4 branches/fibre.

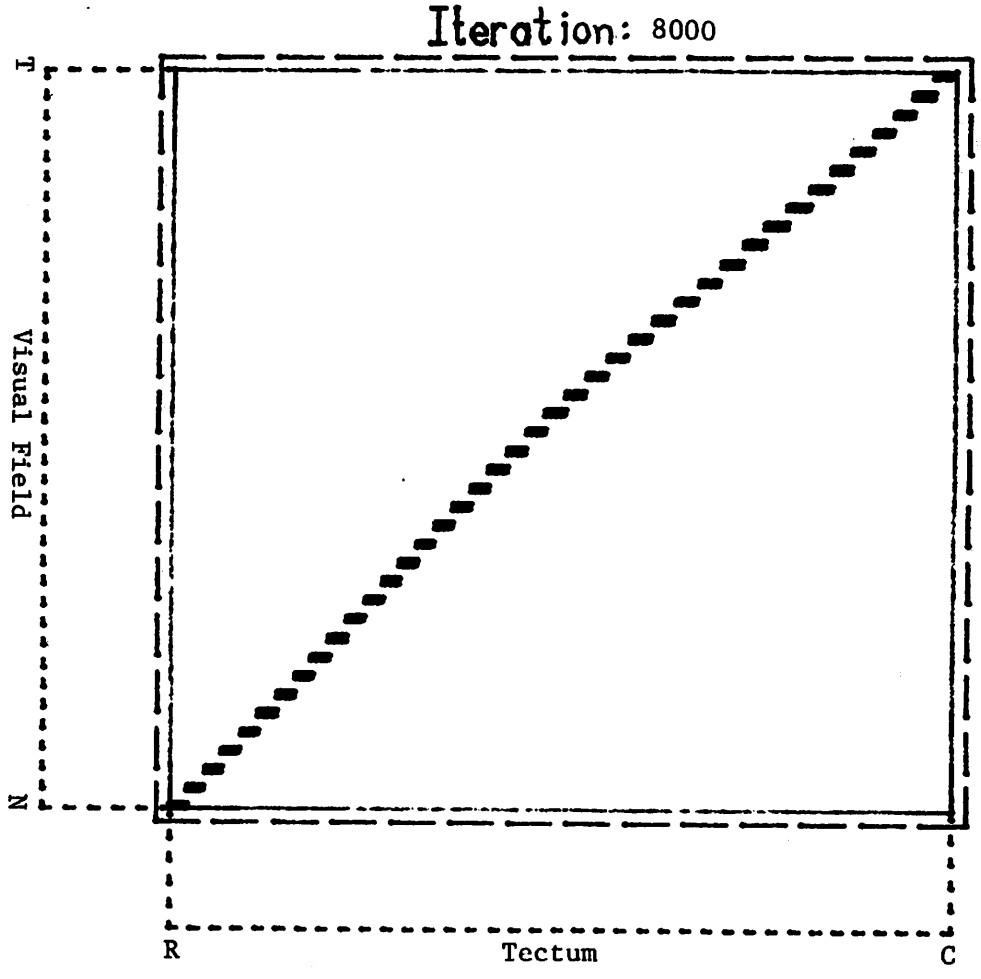

Figure IV.2b Organization of the mapping after 8000 iterations of BAM using a retinal infomation exchange distance equal to the entire extent of the retina.

IV.3c shows the map resulting when the distance is reduced to one fifth of the retinal size. Again, several organized pieces are seen. With the radius reduced to one tenth, the configuration in Figure IV.3d results. The map contains many small pockets of organization yet lacks global organization. The final subfigure, Figure IV.3e shows the resulting map when the retinal interaction distance is reduced to approximately one twentieth of the total retinal expanse. Some areas of organization can be seen, however, no global organization is apparent.

Figure IV.3

This experiment demonstrates that as the distance on the retina within which an effective exchange of information can take place is reduced, the amount of global organization is also reduced. The Arrow Model is essentially the discrete analog of the Branch-Arrow Model when the retinal interaction distance in the latter is equal to the width of the retina. It seems to us that the physiology of the visual systems being studied would indicate that an assumption of effective communication between any two retinal cells regardless of their separation is questionable. Alternately, the distance should be reduced to some fraction of the total width. The exact amount is unknown. The lack of global organization which results when the distance is reduced is evidence that a local neighbourhood interaction mechanism alone is insufficient to account for the organizational behavior observed in the physiological experiments. This point will be addressed in greater detail in the section dealing with XBAM. In the remainder of the experiments with BAM, the distance is assumed to be equal to the width of the retina.

Experiment III.

Work has also been conducted in regard to the compression of the projection onto tectum of which one half has been completely ablated. Udin (1977) and others (Sharma 1977)(Yoon 1976) have studied the form of the retina-tectal projection in such a paradigm in the frog visual system. The results obtained from these experiments are generally consistent. An ordered mapping of the entire visual field is found on the intact portion of the tectum. The projection is compressed to fill the available space. The physiological results are displayed in Figure IV.4, from (Udin 1977).

Figure IV.4

The key features to note here are the facts that the entire visual field is represented along the dimension where only half of the original surface remains and that along the other dimension, all of the space is utilized.

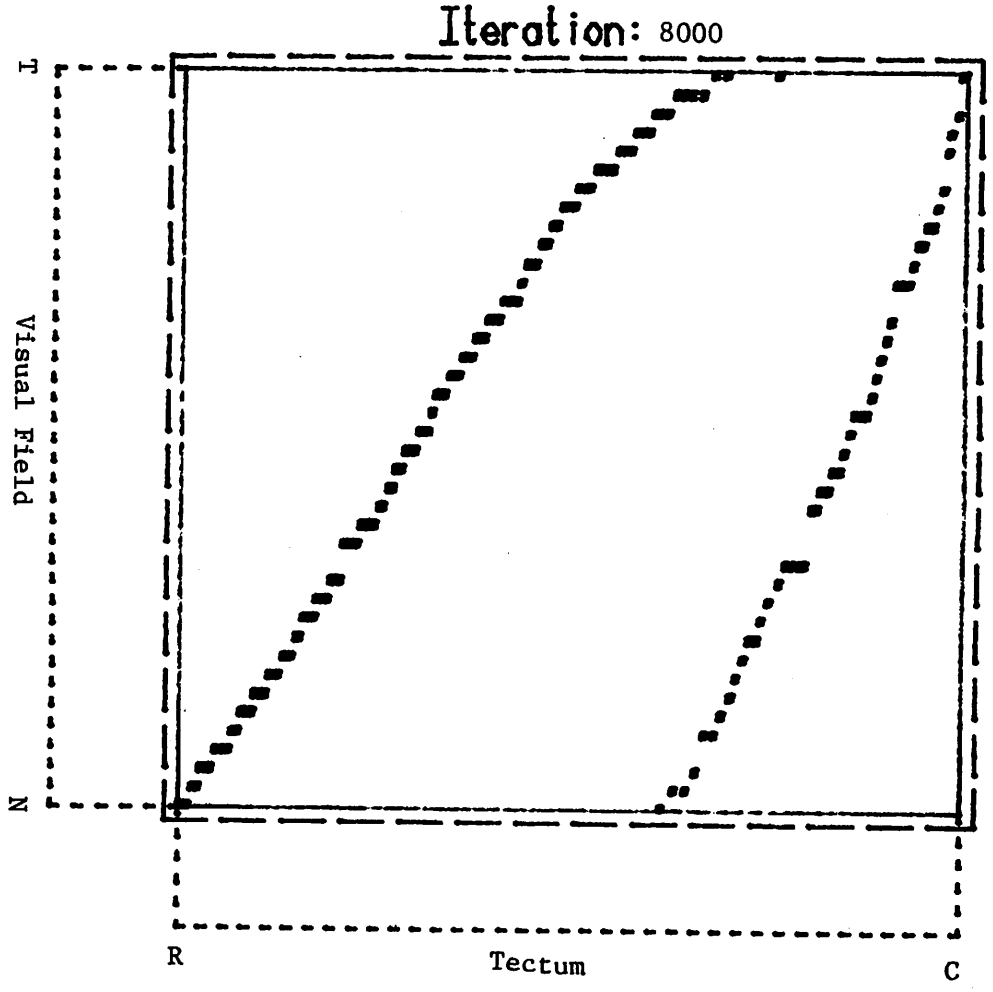

Figure IV.3a Organization of the mapping after 8000 iterations of BAM with the distance on the retina allowing an effective exchange of information reduced to roughly 2/3 of the retina width.

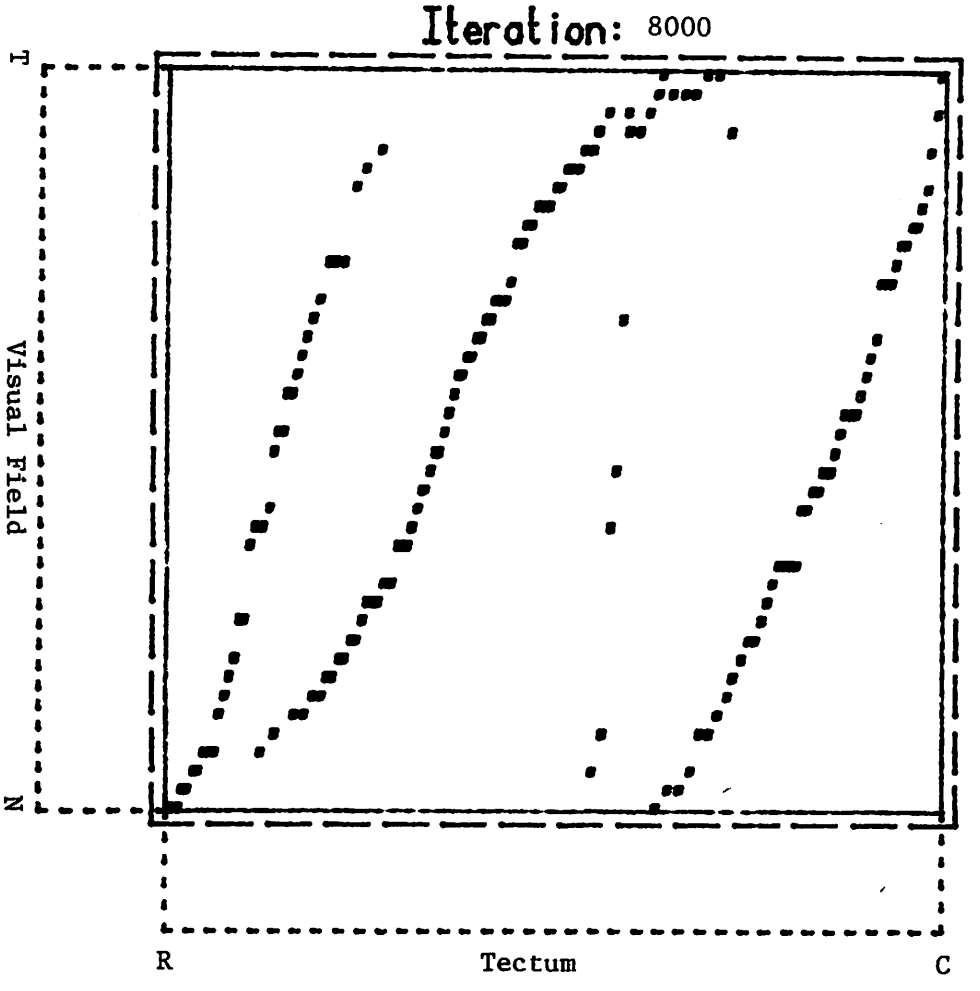

Figure IV.3b State of the mapping after 8000 iterations of BAM with the retinal interaction distance reduced to 1/2 of the retina width.

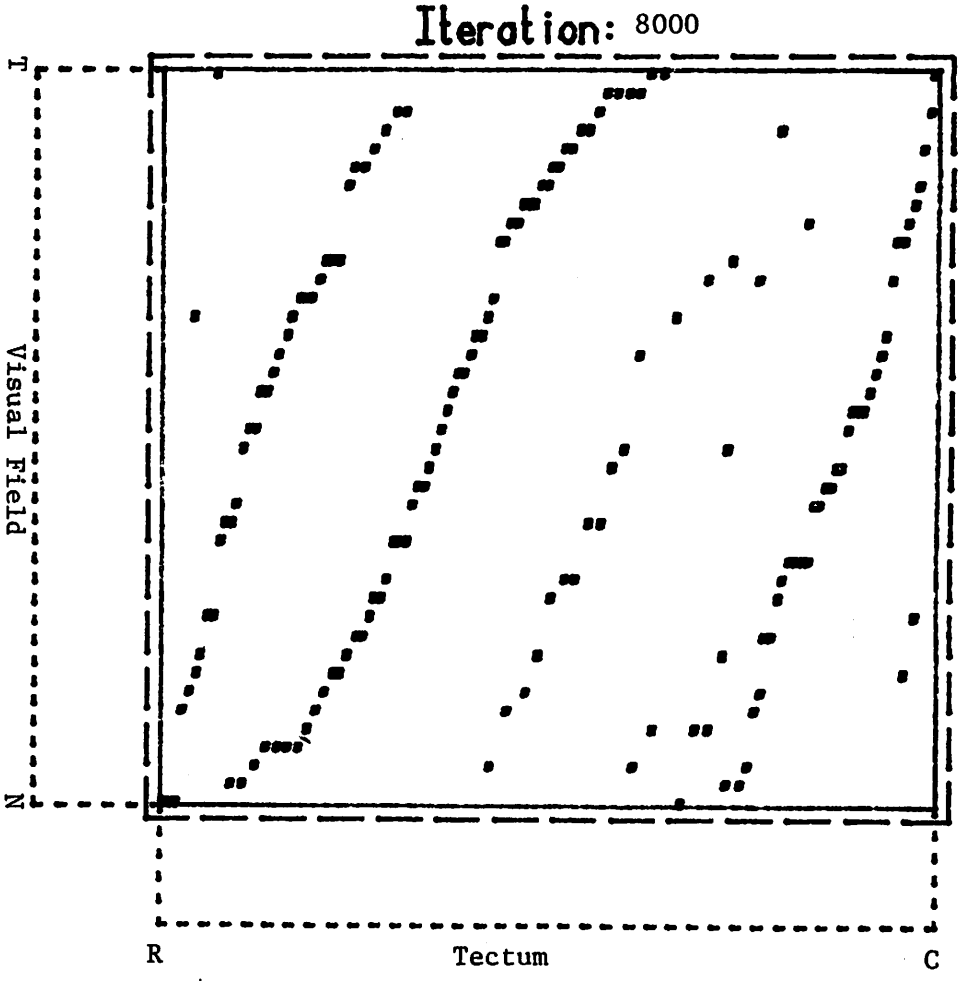

Figure IV.3c Organization after 8000 iterations of BAM, retinal information exchange distance reduced to 1/5 of the retinal width.

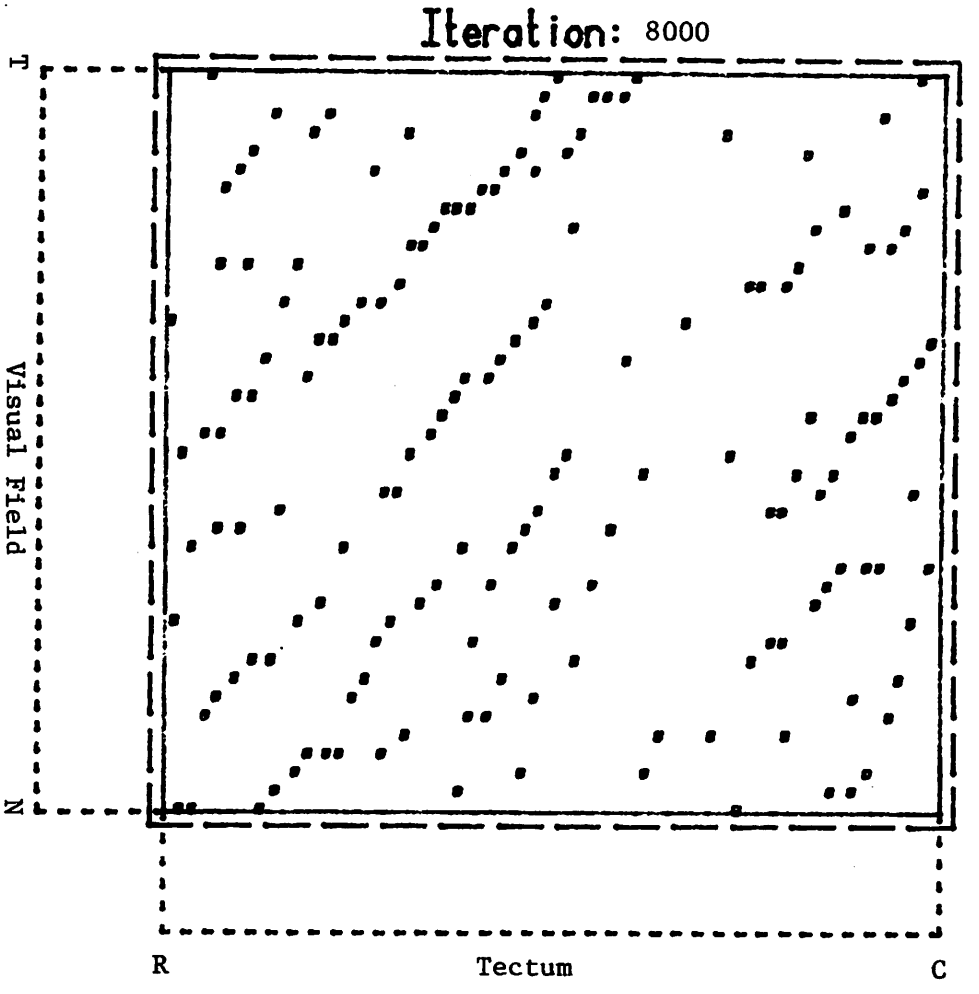

Figure IV.3d Organization after 8000 iterations of BAM, retinal information exchange distance equal to 1/10 of the total retina width.

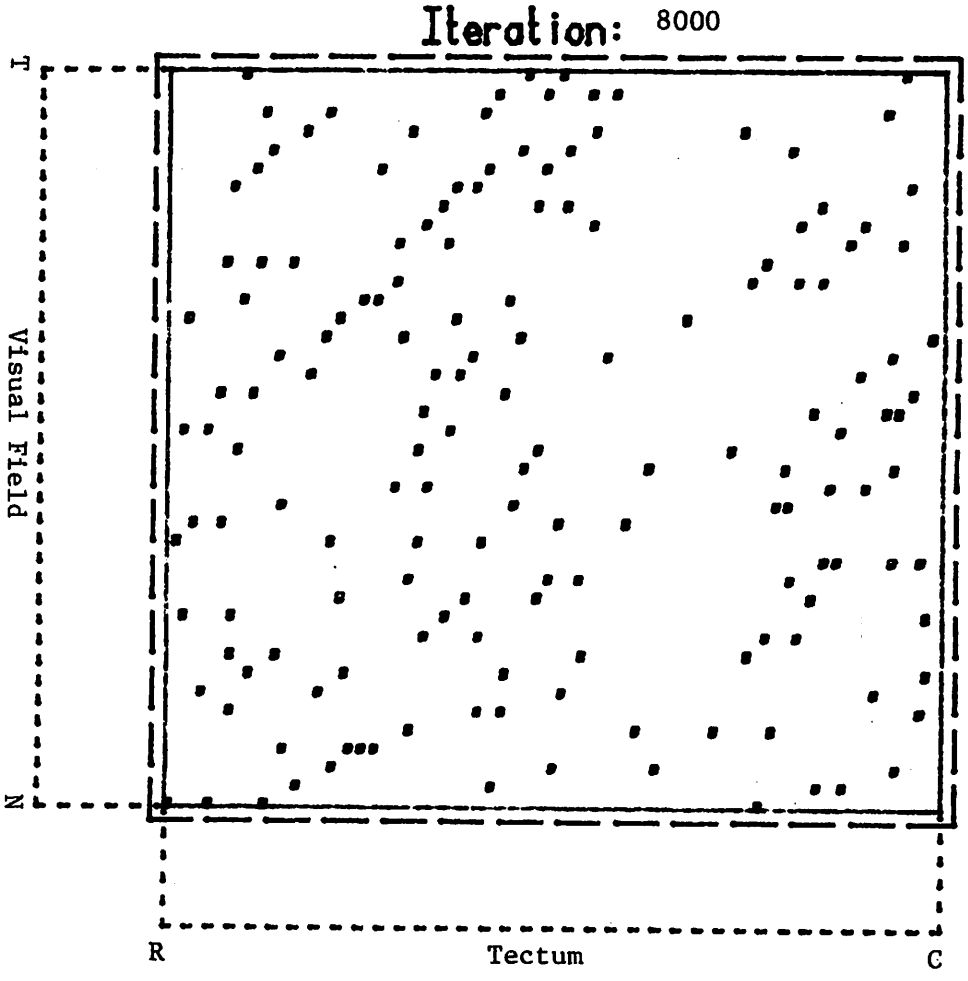

Figure IV.3e Organization after 8000 iterations of BAM, retinal distance equal to 1/20 of the retina width. No global organization is apparent.

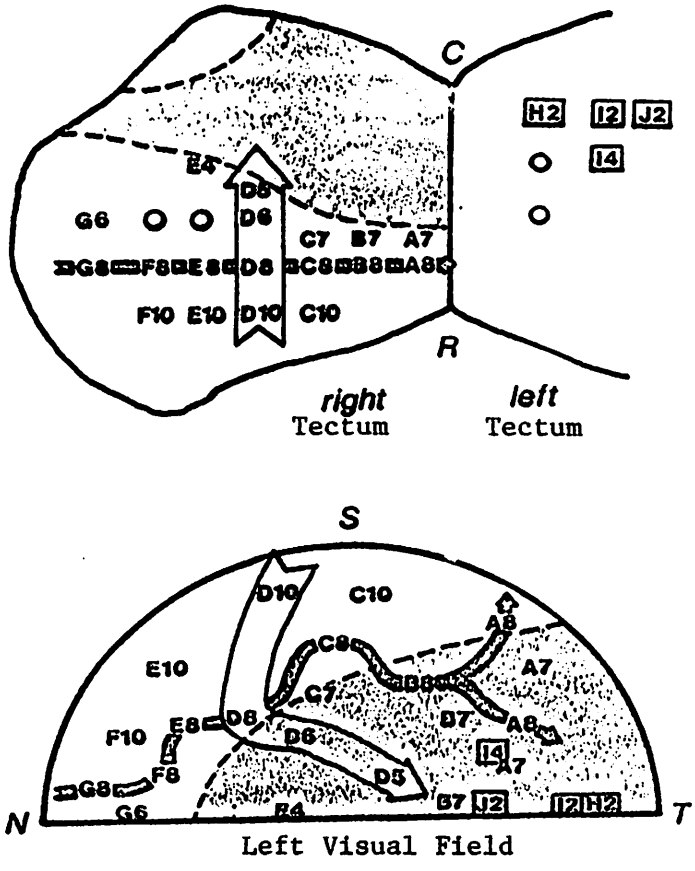

Figure IV.4 Physiological data from caudal 1/2 tectal ablation experiment (Udin 1977). The mapping from the entire visual field is compressed onto the remaining tectal surface.

Figure IV.5 contains the results from the computer simulation. The initial termination locations were randomly distributed over the tectal surface. For this experiment, the surface was reduced to half of its original size. All simulation other parameters were defined as in the previous two experiments. The organization of the projection after 8000 iterations is shown in the figure. This map shows excellent global organization. The branches in the extreme lower left portion of the field have been forced off of the tectal surface. The magnitude of the effect is determined in part by the relative magnitudes of the unit movement vector and the boundary strength parameter in the particular simulation run.

Figure IV.5

Some investigators have noticed that a mapping identical to the original mapping with the normal tectum appears first, followed by a trend toward a complete, compressed projection (Sharma 1977) (Cook 1974). Horder (1977) found duplicate maps initially which later appeared compressed. He further found that if one third or less of the surface was ablated, the projection moved immediately to a compressed state. It has been posited that this initial mapping is due, in part, to the debris left on the tectum when the optic nerve is sectioned and then degenerates. The fibres which originally mapped to the rostral half of the tectum may be guided by the debris remaining from the prior mapping. Sharma (Sharma 1977) performed an experiment to test this hypothesis and found that when the fibres are forced to reinnervate a tectum previously devoid of fibres, the compressed mapping appeared with no initially uncompressed projection.

Another tectal ablation experiment involves removing 1/4 of the tectal surface and mapping the projection after regeneration. Schmidt and Easter (1978c) have performed experiments in which the medial-caudal quarter of the left tectum of the goldfish has been surgically ablated. A similar experiment designed to investigate the effect of removing part of the tectal surface was performed by Sharma (1972) and involved the ablation of a rostroventral strip on the tectal surface. An organized mapping was found compressed onto the remaining surface. The purpose of these experiments was to determin the degree to which the axes of the tectum are independent with respect to the compression of the mapping. They found that, after reinnervation of the tectum, the entire visual field was represented on the tectum. Further, the mapping was completely ordered and was compressed with respect to both axes. The compression appears to have been uniform across the tectum, that is, the fibre arbors appeared to organize in a fashion which resulted not only in an ordered representation of the visual field but also in a uniform distribution across the available tectal surface. While we cannot duplicate this paradigm due to the one dimensional nature of our simulation, we can predict the behavior of the two dimension version of the model in such a case.

Since our model tends to minimize the overlap of adjacent projection fields, as illustrated in the compression results above, and produces a continuous mapping, we would predict that the projection resulting when 1/4 of the tectal surface is removed would be uniformly compressed in all directions.

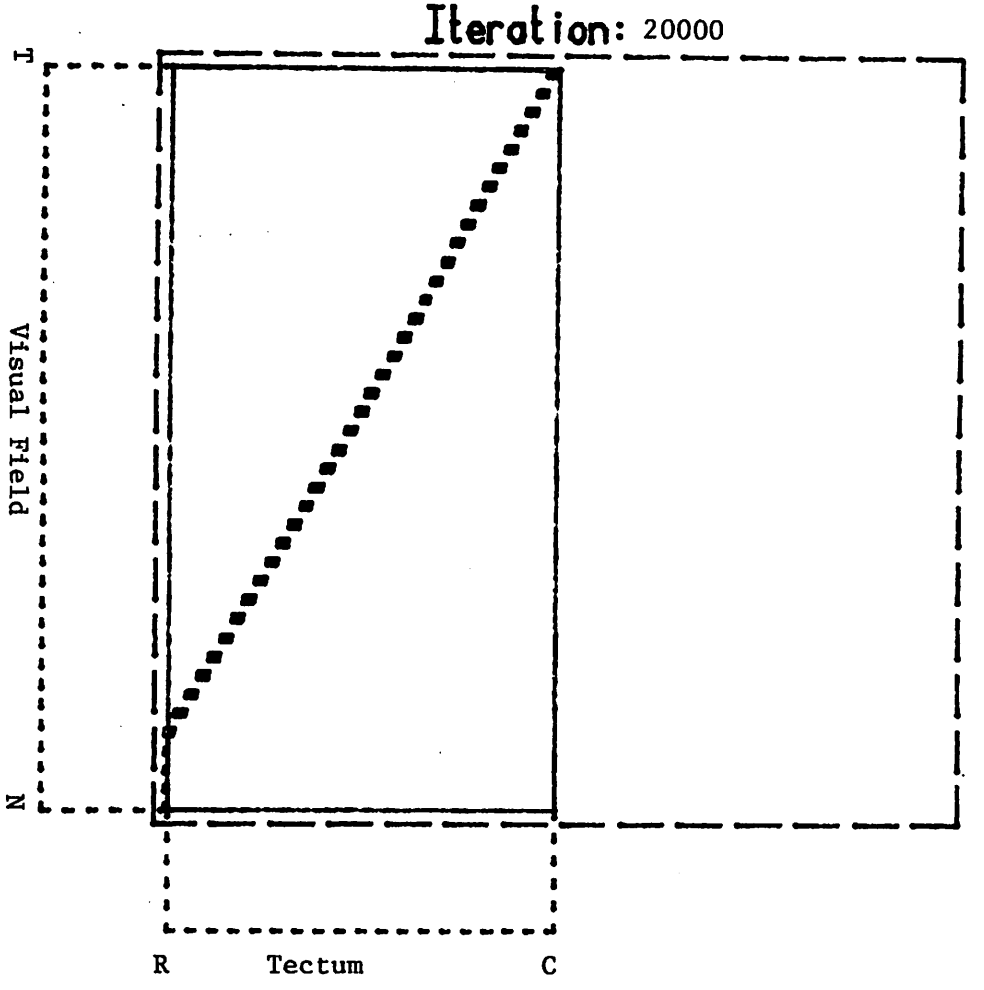

Figure IV.5 Results after 20000 iterations of the BAM simulation in which the entire retina is forced to map onto a tectum which is only 1/2 the size of that in a normal projection.

Experiment IV.

Another class of experiments involves studies of the map resulting between a hemiretina and an intact tectum (Schmidt 1978a) (Horder 1971). In this case, the projection of the half of the visual field represented on the remaining hemiretina expands in an orderly manner to completely fill the available space on the tectum. Typical results are found in Figure IV.6, from (Schmidt 1978b). Feldman (1975) conducted an experiment in which one eye was removed before it differentiated and the fibres from the other eye were directed to the ipsilateral tectum. He found a normal projection of the entire visual field on the ipsilateral tectum. However, some of the retinal fibres had managed to innervate the contralateral tectum to produce an expanded projection of the represented area of the visual field.

Figure IV.6

The simulation results for this situation are given in Figure IV.7. The initial locations for the branches were randomly assigned. The state after 24000 iterations shows complete organization with half of the normal number of fibres mapping onto the complete tectal surface.

Figure IV.7

Figure IV.7b illustrates the results of a related experiment. Again half of the retinal surface has been ablated. In addition, the half of the tectal surface to which the remaining retinal surface should project has been ablated. Thus the projection from the retina is to the foreign half of the tectum. The preojection shows complete organization. This result is expected since the BAM does not contain information about the specific labelling of the tectal surface, only information describing relative orientation.

Experiment V.

A direct extension to the hemiretina, full tectum experiments involves studying the projection resulting when hemiretinae from different eyes are fused to form a single eye. Once the nerve connections have regenerated, the mapping is determined electrophysiologically. Gaze et al (1963, 1965) and Hunt (1973) have conducted such experiments. Their results are shown in Figure IV.8.

Figure IV.8

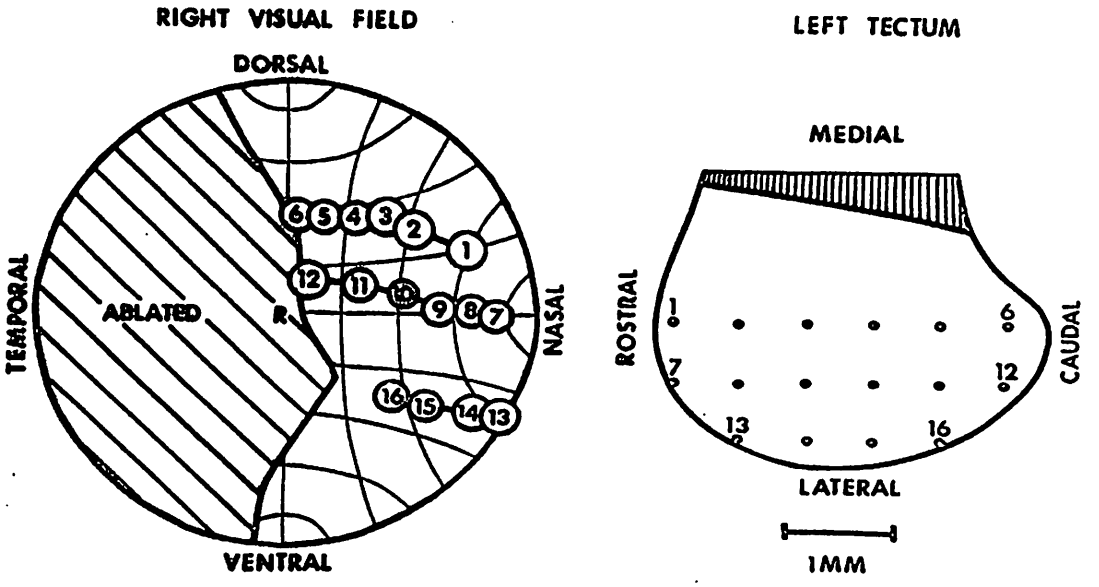

Figure IV.6 Physiological data from an animal in which the nasal half of the retina has been ablated. The remaining visual field is represented by an ordered projection covering all of the tectal surface. (Schmidt 1978b)

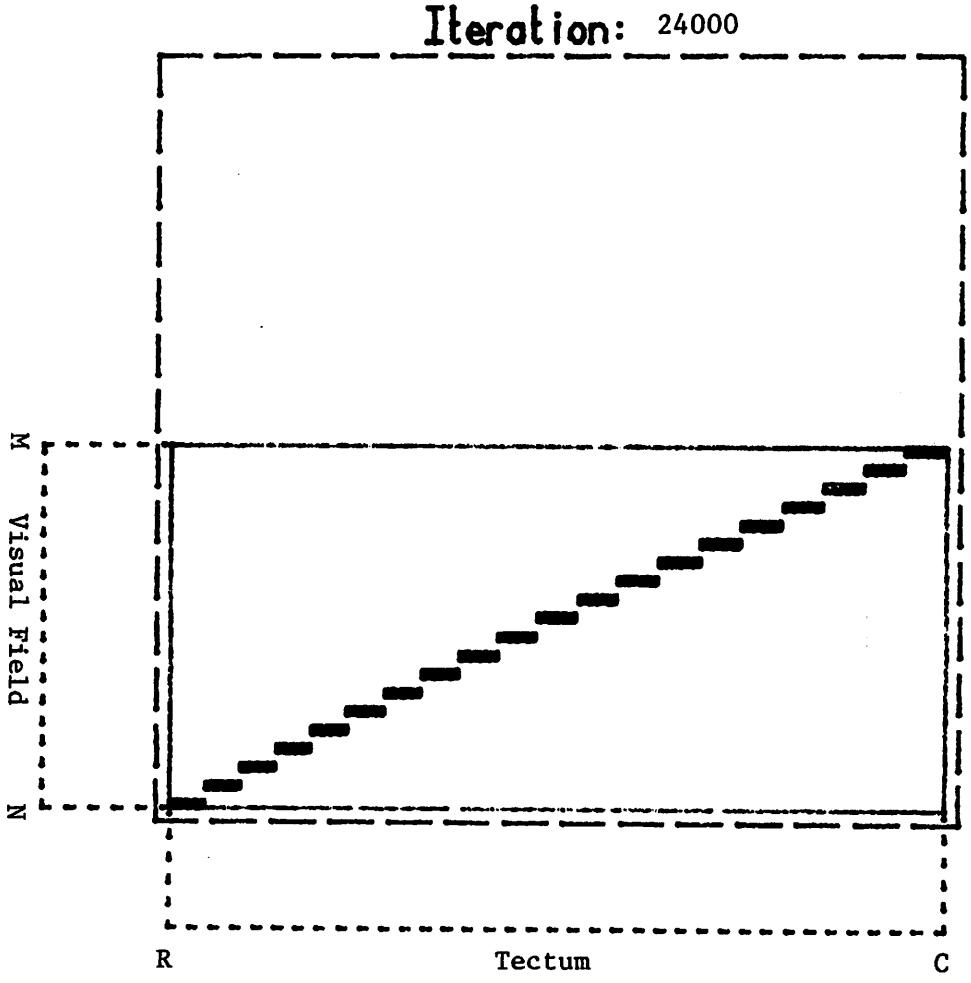

Figure IV.7a Configuration of the projection from a retina 1/2 of the normal size onto a full tectum after 24000 iterations of BAM.

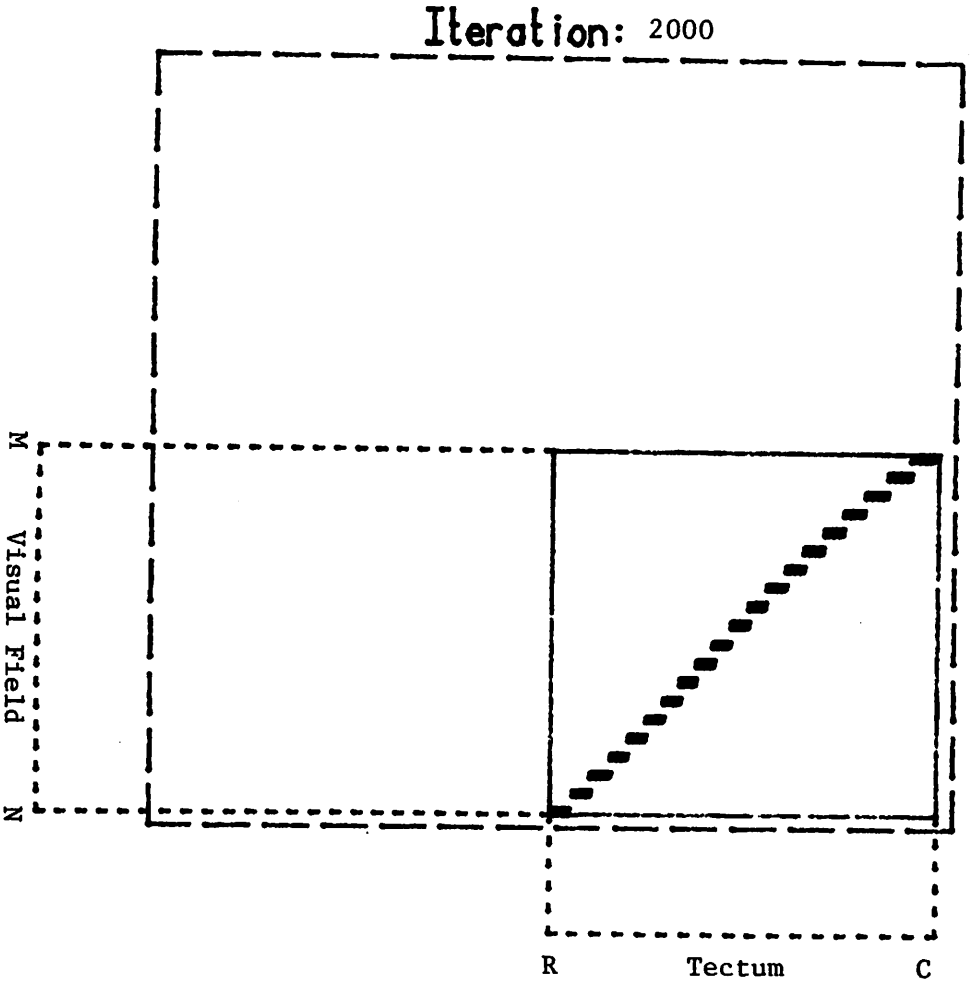

Figure IV.7b Simulation results in the case where a hemiretina projects onto the "wrong" half tectum. That is, this half of the retina normally projects onto the other half of the tectum. Results after 2000 iterations of BAM.

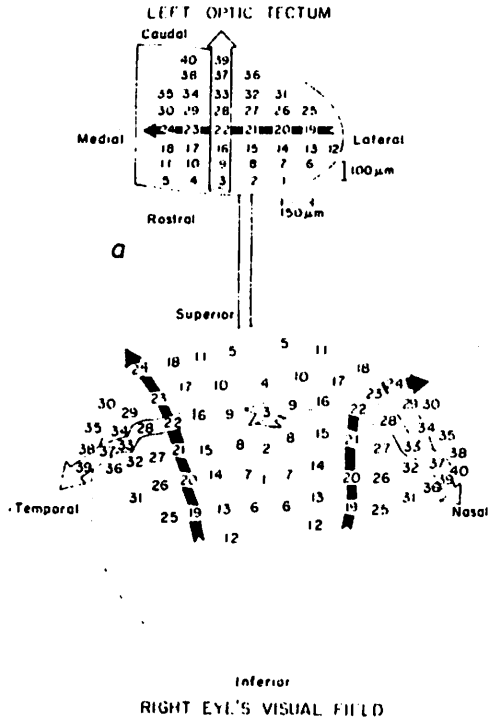

Figure IV.8a Projection of the visual field from a double-nasal compound eye onto a normal tectum (Hunt 1973). Notice that there are two overlapping projections, one from each half of the eye.

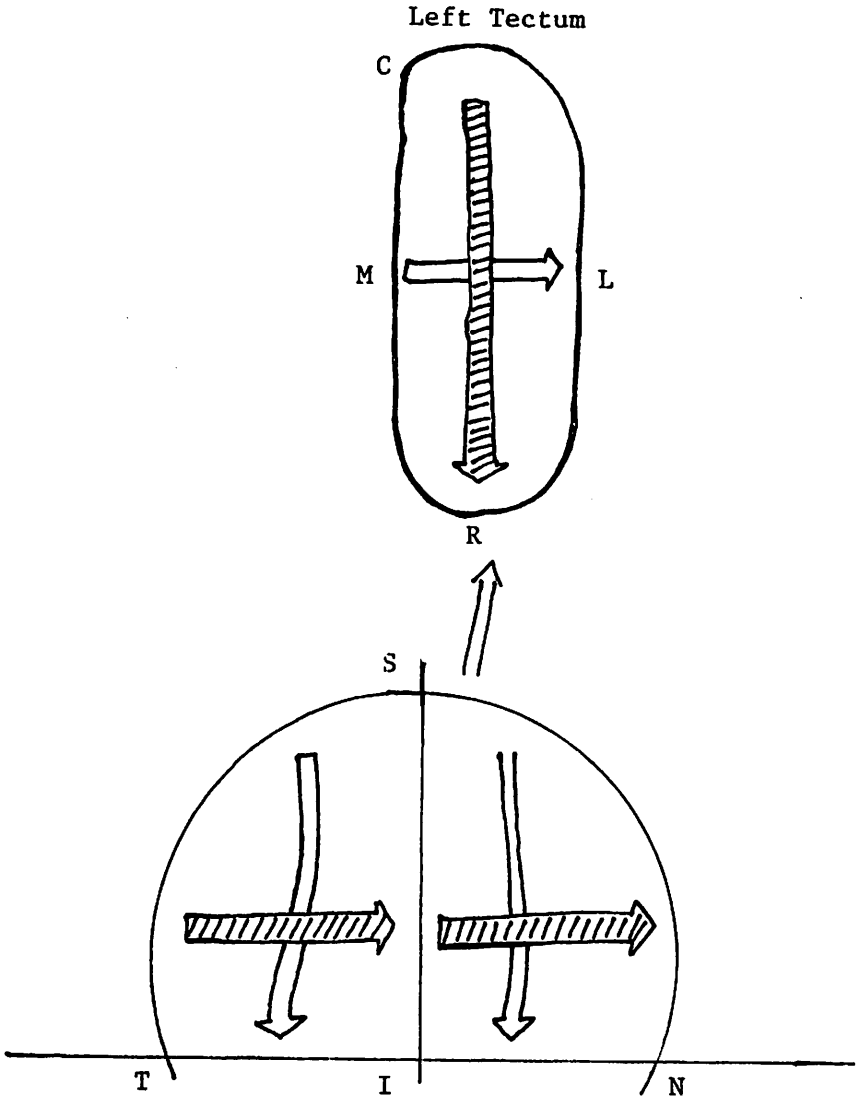

Figure IV.8b Schematic of the projection resulting from a compound eye composed of the nasal hemiretina from one eye and the temporal hemiretina from another.

In the case of Figure IV.8a, (Hunt 1973), the compound eye was composed of the nasal hemiretinae of two eyes with the division along the superior-inferior axis. The interesting point to note is that the projection from the two halves of the compound eye are superimposed. That is, the projection from each hemiretina expanded in an organized way to cover the entire tectal surface. The projection from one of the hemiretina is rotated 180 degrees. This is the case since one of the hemiretinae had to rotated through 180 degrees in order to create the complete eye. Figure IV.8b contains a schematic of the results from a compound eye composed of two temporal hemiretinae. The projections are ordered the same since the neither piece required rotation when the eye was constructed.

Figure IV.9 contains the results from computer simulations of the BAM under similar circumstances. Figure IV.9a was produced with the orientation of one piece reversed. Figure IV.9b results from hemiretinae with their orientations retained so that the maps are oriented the same. Recall that the simulation proceeds from a known retina and visual field, and the results are depicted in terms of the organization on the tectum. Also, the simulation is one dimensional.

Figure IV.9

Notice that in both cases the global organization of the field represented on each hemiretinae is maintained. However, the projection has expanded to cover the entire available tectal surface. This result is expected in the systems matching paradigm if it is assumed that the exchange of information between retinal cells separated by the junction of the two hemiretinae is negligible or random at best.

To this point, the experiments have focused on the mappings when there is a mismatch in the size or type (e.g. the compound eye experiments) of retinal versus tectal tissue. Another class of experiments involves the excision of a section of the tectum and its subsequent reimplantation after some form of inversion or rotation. Yoon (1975) and Sharma and Gaze (1971) have studied the projection following a 90 degree rotation of the graft tissue about the dorsoventral axis. Completely ordered projections are found both within and surrounding the graft. The projection within the graft, however, is found to be rotated in the same manner relative the the tectum as the graft. Figure IV.10, taken from (Yoon 1975) illustrates these results.

Figure IV.10

Several neurophysiologists (Yoon 1973, 1975) (Levine 1974) have experimented with animals in which a single tectal graft has been rotated 180 degrees, again about the dorsoventral axis. Once the tectum has been reinnervated the mapping is found to be completely ordered both within and around the graft. The orientation of the map within the graft is again found to be rotated in a manner identical to the graft, see Figure IV.11, again from (Yoon 1975).

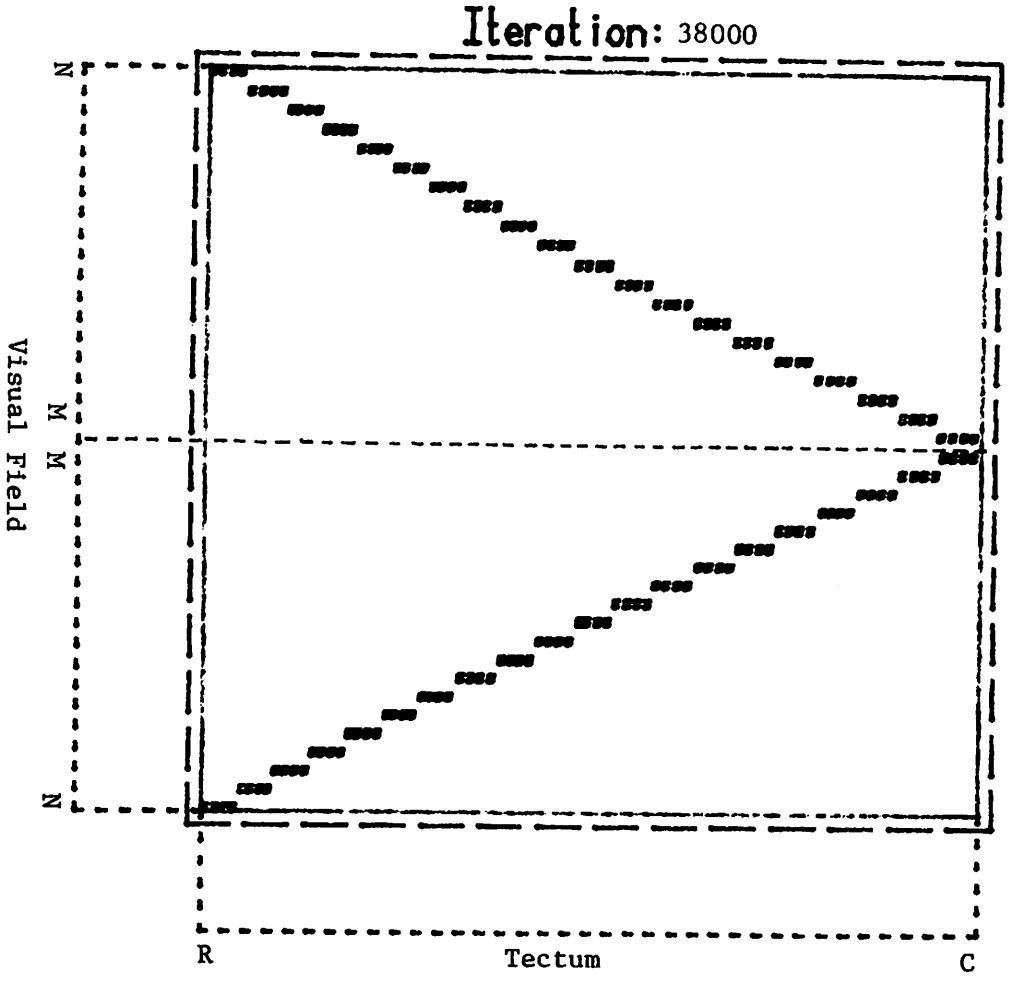

Figure IV.9a Simulation results of the double-nasal compound eye experiement. 38000 iterations.

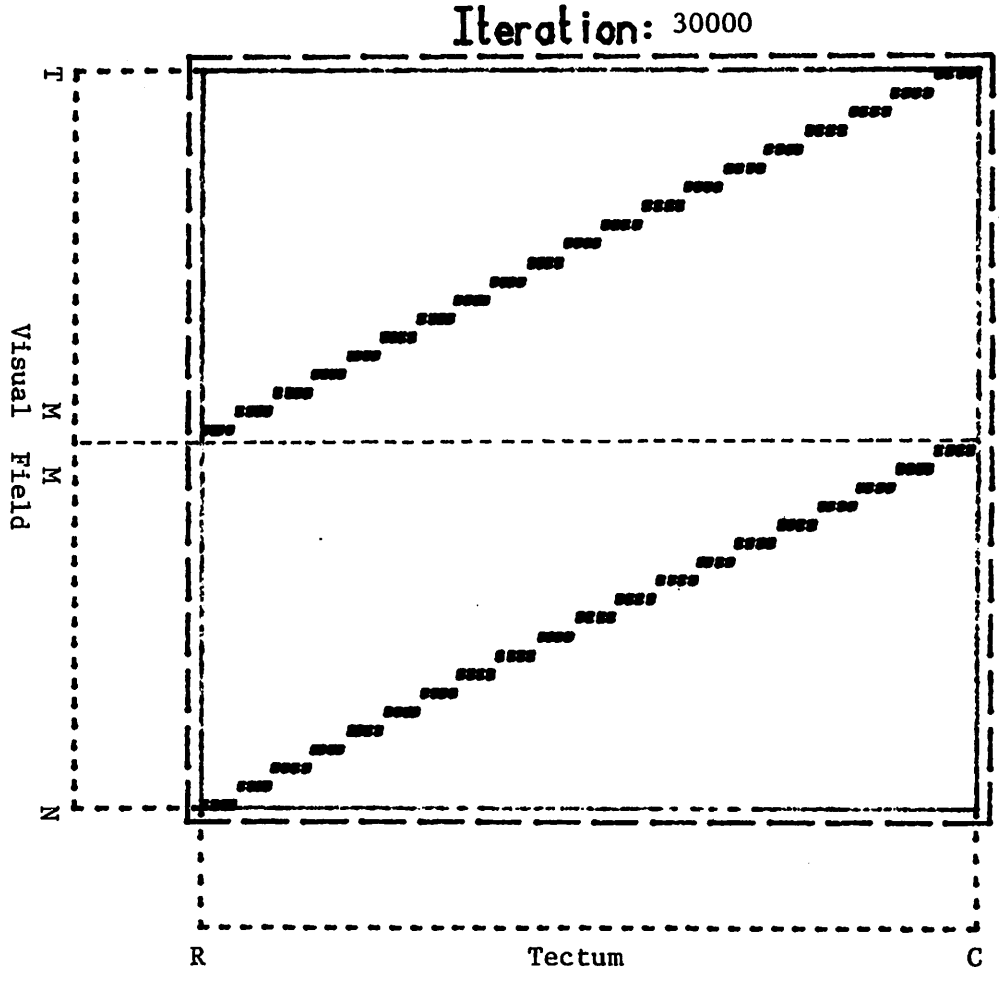

Figure IV.9b Simulation of the nasal-temporal compound eye. 30000 iterations.

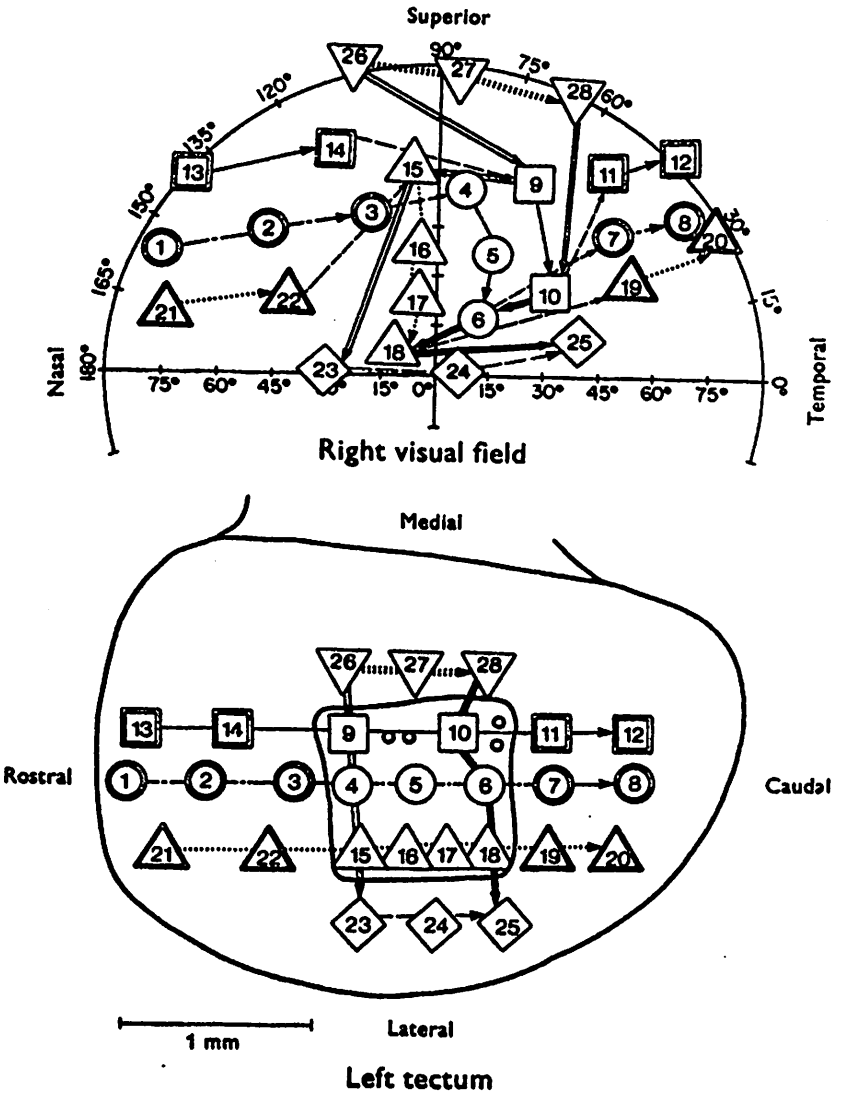

Figure IV.10 Mapping recorded after section of the optic nerve and 90 degree counterclockwise rotation of a graft (Yoon 1975).

Figure IV.11

Yoon (1975) has also performed experiments in which a graft has been excised, rotated 180 degrees about the rostocaudal axis, and reimplanted. This rotation causes the graft to retain its normal orientation along the rostocaudal axis while having an inverted orientation along the superior-inferior axis. The resulting projection map is illustrated in Figure IV.12, (Yoon 1975), and shows that the map retains its normal rostocaudal organization while the mediolateral organization within the graft is reversed. Again, the local orientation of the map follows that of the underlying tectal surface.

Figure IV.12

Experiment VI.

Since the Simulation of the BAM is one dimensional, the 90 degree rotation experiments cannot be performed and the two forms of the 180 degree rotations are equivalent. Figure IV.13 illustrates the state of organization of the branch termination locations after 8000 iterations. The initial configuration was again random.

Figure IV.13

The areas both within and surrounding the graft are organized. However, it is interesting to note that the entire visual field is represented in each of the three sections. Ideally, only the central portion of the visual field should be represented within the graft. This behavior is due to the interaction mechanism employed by the model and is an inherent difficulty.

Consider a branch located at the left most edge of the graft. The influence felt from the branches to its right tends to force the branch to move to the left while the opposite is true for the branches located immediately to the left, off the graft. Thus the branch is held at the edge of the graft. With this interplay at the graft boundaries, it is impossible for a branch to move across the graft to its proper side.

Experiment VII.

The previous experiment illustrated that the simple BAM cannot produce behavior exactly as that found in graft rotation experiments. This experiment emphasizes this point more dramatically.

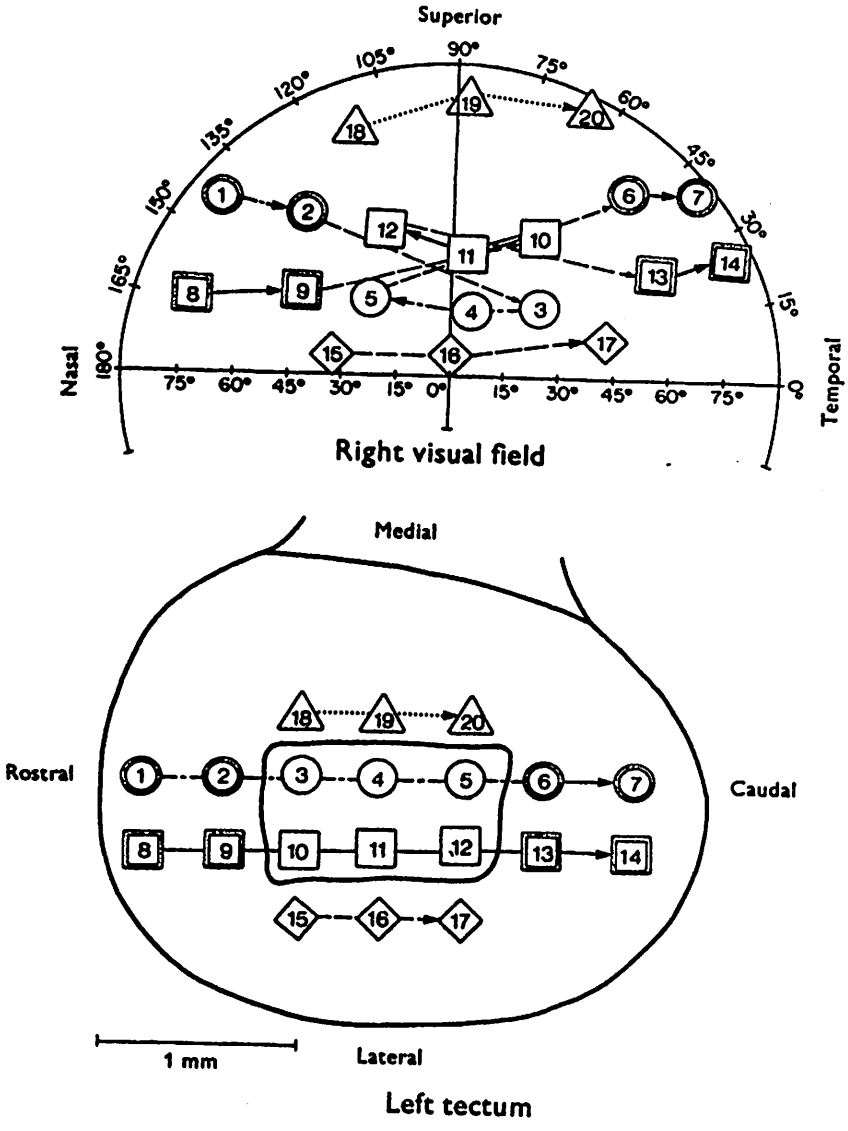

Figure IV.11 Visual field projection organization after optic nerve section and 180 degree rotation about the dorsoventral axis of a graft (Yoon 1975).

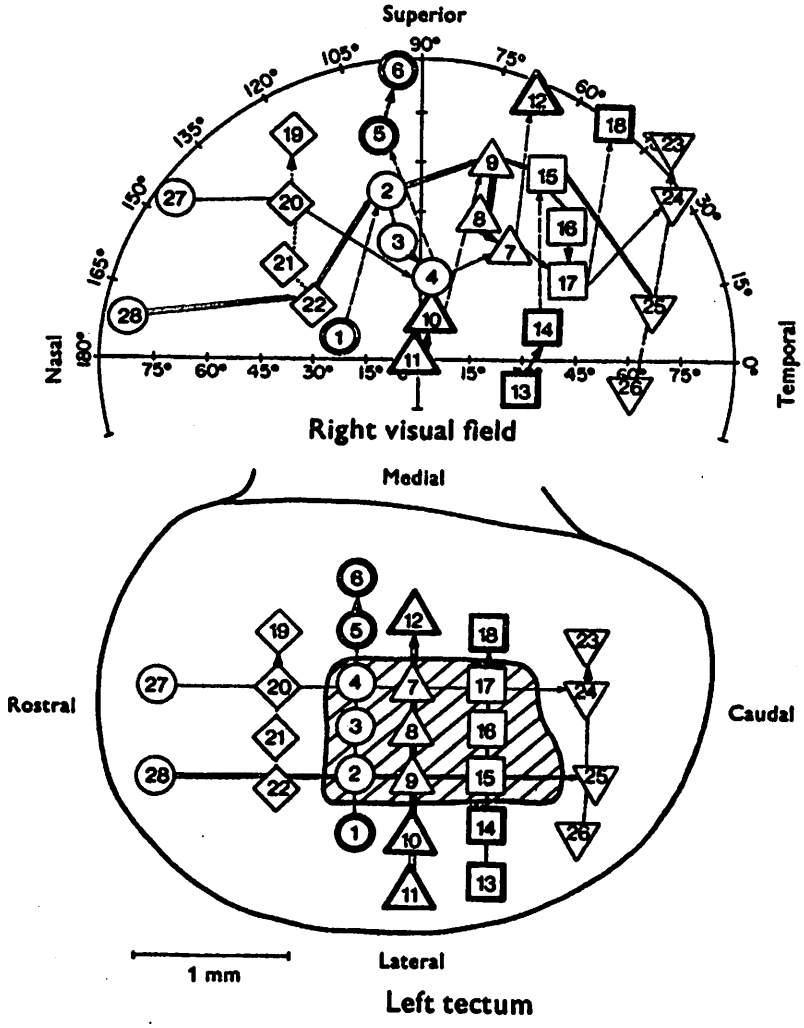

Figure IV.12 Projection organization after optic nerve section and graft inversion along the rostrocaudal axis (Yoon 1975).

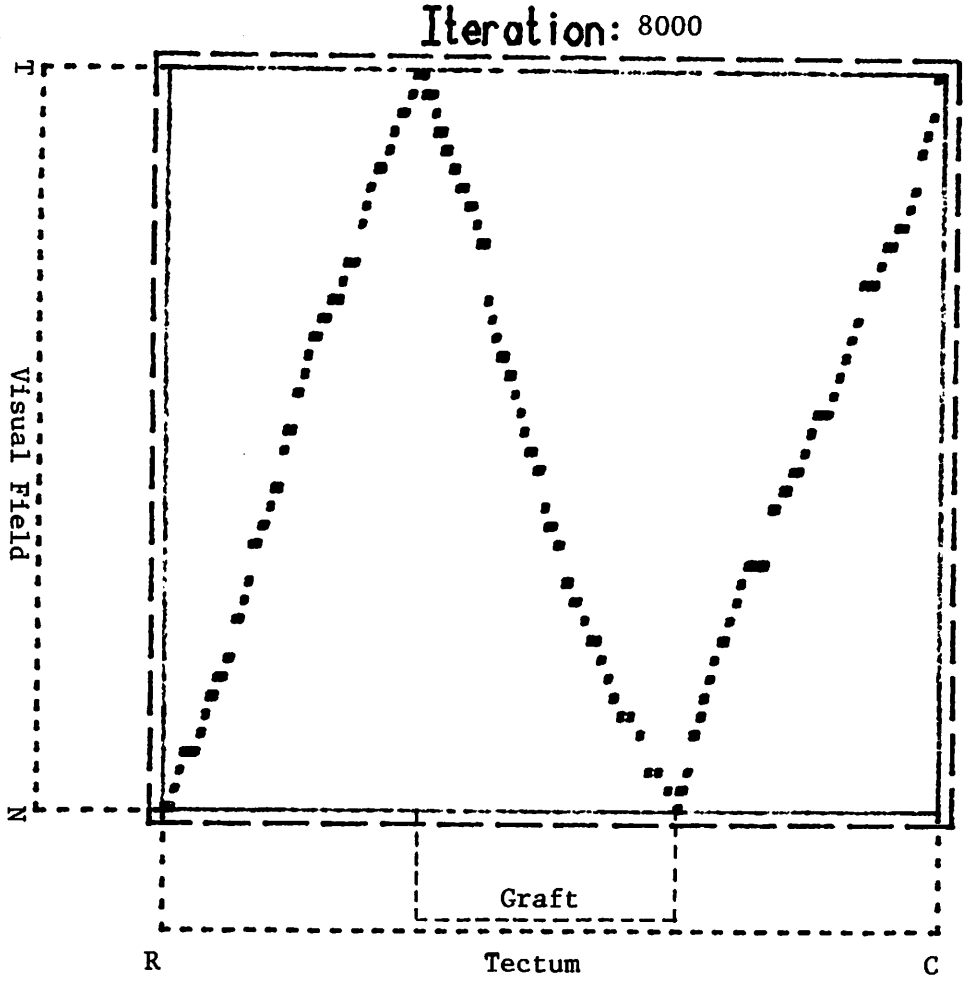

Figure IV.13 Results of 8000 iterations of BAM in the case of a single enverted graft. Notice that the entire visual field is represented in each of the three sections and that the organization within each section is ordered.

An extension to the graft rotation experiments consists of excising two pieces of tissue from the surface of the tectum and reimplanting them without rotation yet with their positions switched, (Hope 1976). This is a difficult experiment to perform physiologically and the few available results are not totally consistent. In some cases, a completely normal projection is seen. This result would favor the "systems matching" theory of organization. However, different results have been obtained. In these cases the projection is ordered both within and surrounding the grafts but the grafts retain their original spatial mapping. Thus two sections of the mapping are interchanged. Since no information is available to differentiate between two tectal locations, these data support the "point-to-point chemospecificity" approach. Physiological results from such experiments are given in Figure IV.14, from (Hope 1976).

Figure IV.14

Simulation results from this situation appear in Figure IV.15. Note that the projection is organized as in the case of a normal tectal surface, compare with Figure IV.2b. This result is expected since the model contains information allowing only direction determination on the tectum, not absolute position of individual locations.

Figure IV.15

Experiment VIII.

This experiment was designed to emulate two particular points in the development of the retina and tectum. All of the experiments outlined above used an initial configuration which consisted of the initial termination locations being randomly distributed over the surface of the tectum. Since the tectum is innervated from the rostromedial area, this assumption is not accurate. Figure IV.16 illustrates the configuration apparent after 20000 iterations with the fibres initially randomly distributed over a very narrow band located toward the left end of the tectal surface.

Figure IV.16

The mapping displays excellent global organization with the "tails" slowly speading to fill all of the available space. If allowed to continue to iterate, a complete mapping identical in structure to that in Figure IV.2b would result.

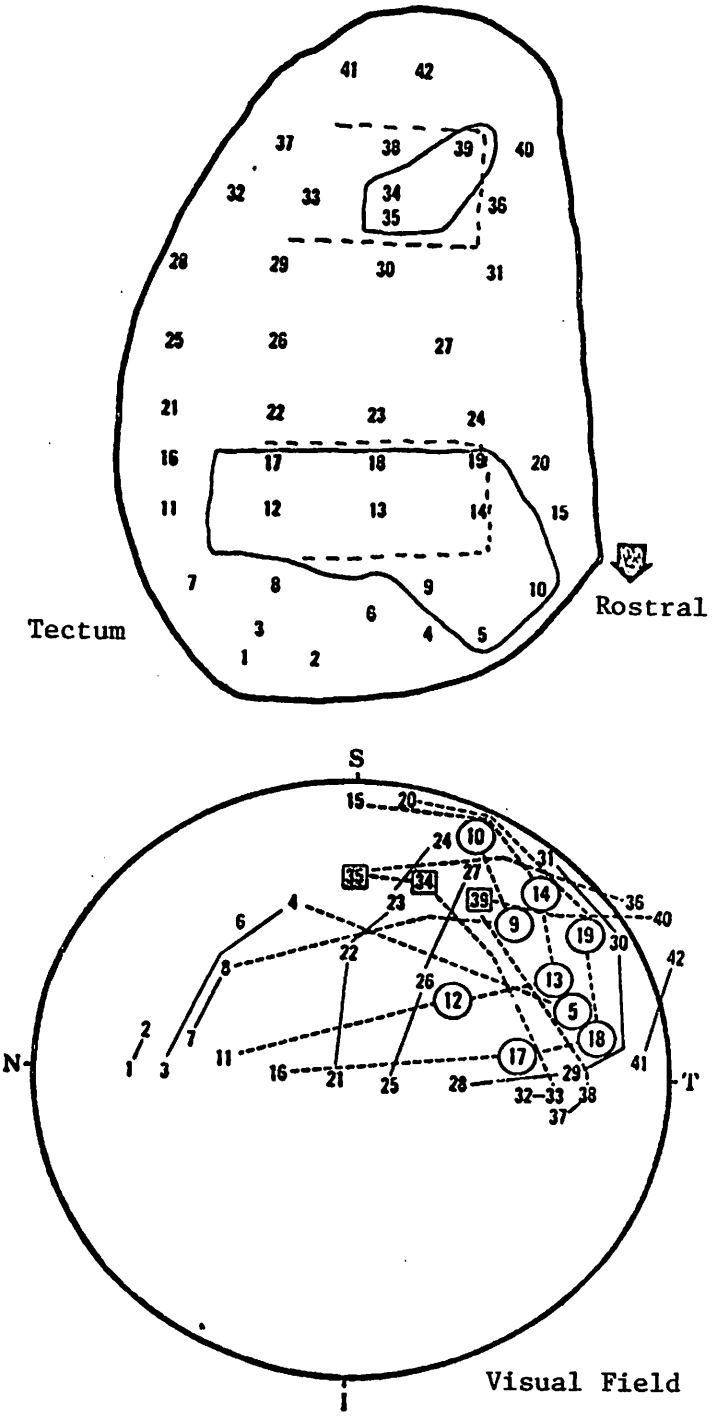

Figure IV.14 Mapping data from an animal with the positions but not orientations changed for two grafts. (Hope 1976)

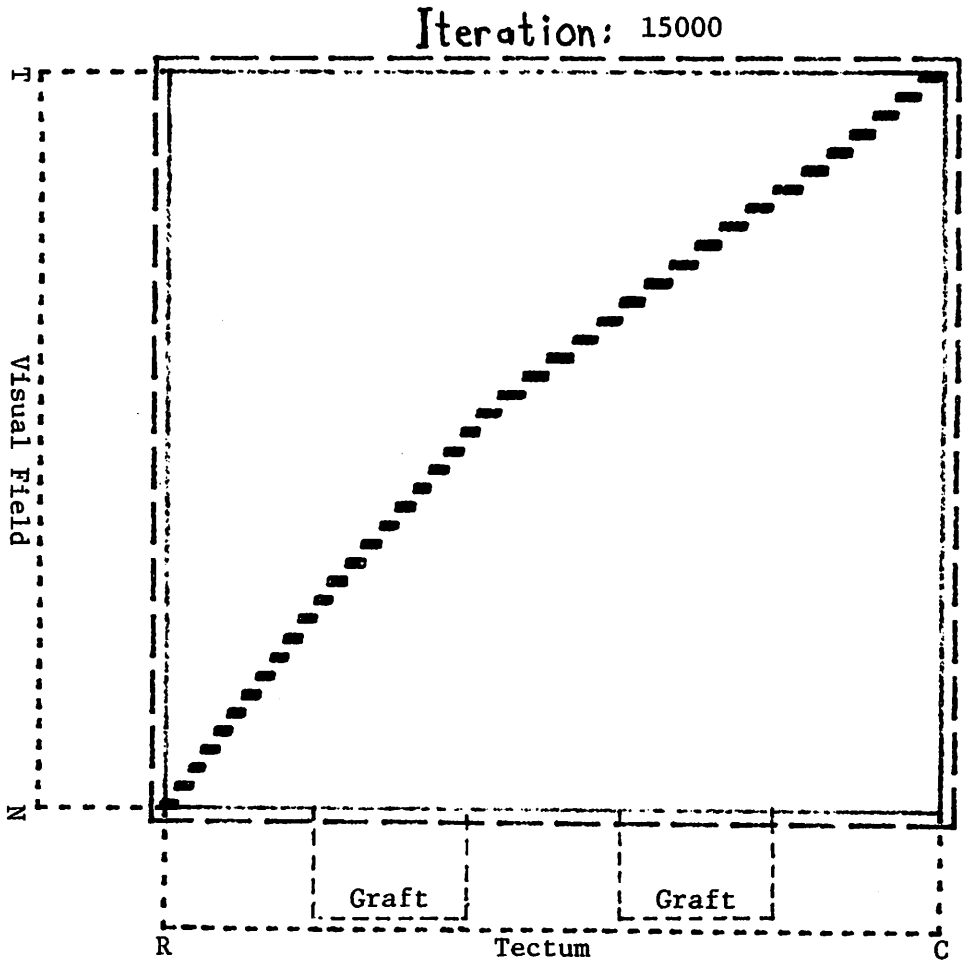

Figure IV.15 BAM simulation results, 32500 iterations, of the paradigm in which two grafts are translocated but their orientations are maintained.

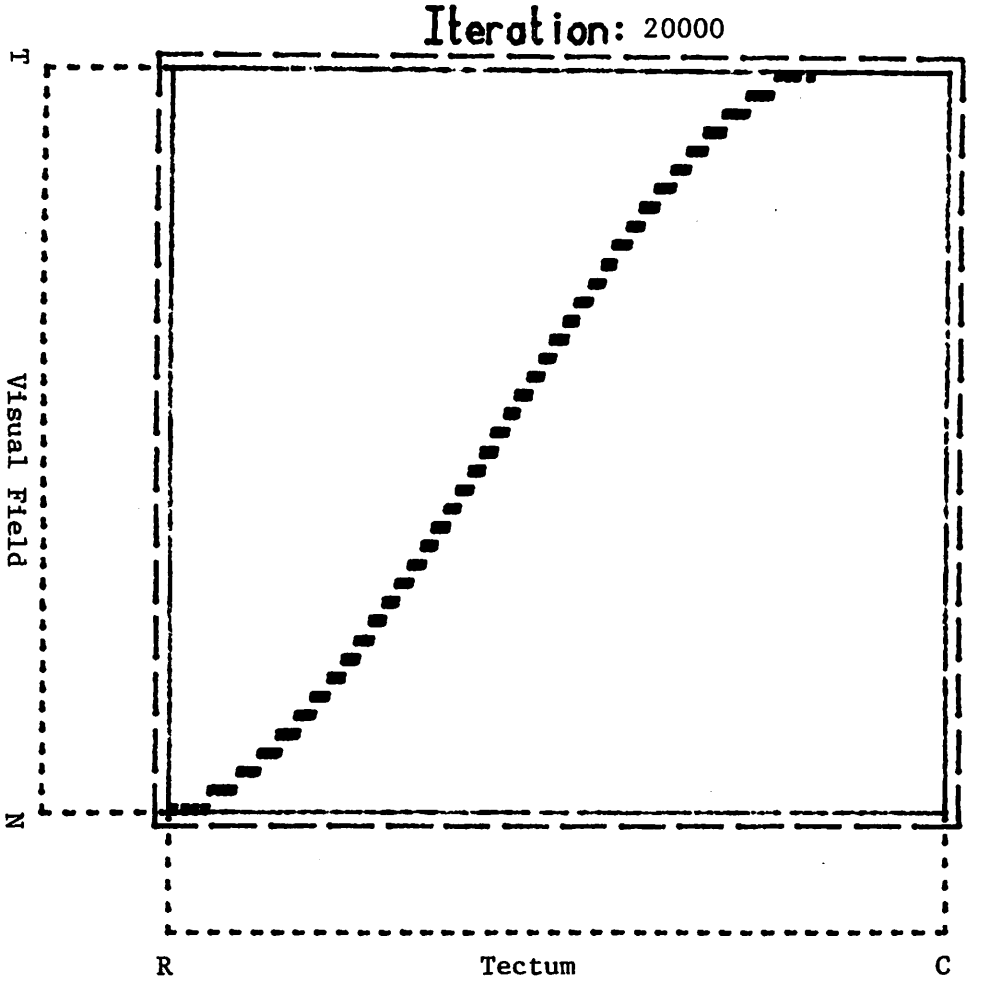

Figure IV.16 BAM simulation results when a normal retina innervates an intact tectum. In this case the branches were distributed initially over a very small section of the tectal surface.

V. The Problem

From Experiments I through VIII with the simulation of BAM, it is apparent that this model, using the principles of system matching, accounts for a great deal of the experimental data. Relative retinal and tectal orientation information is sufficient to produce behavior similar to most of the experimental results when utilized by neighbourhood and boundary interaction mechanisms. If the effect of retinal separation an the ability of two retinal cells to communicate is investigated, as in Experiment II, degraded behavior results. Restricting the distance allowing a meaningful exchange to a fraction of the retinal expanse results in a locally continuous yet globally discontinuous mapping. Experiments VII and VIII illustrated that BAM cannot accurately produce the graft rotation and translocation behavior seen experimentally. The systems matching approach then appears inadequate to account for the physiological data. This is due to the lack of specific information differentiating individual tectal locations and the inability for information to be shared over distances which are large relative to the neighbourhood interaction. This amount of information is insufficient, however, to account for the class of experiments in which the locations but not the orientations are changed for a pair of grafts. Unlike the system matching ideas, point-to-point chemoaffinity provides specific information describing every point on the two surfaces.

Experiment II was designed to demonstrate the effect of varying the retinal distance allowing effective communication between cell somas. The results indicate that any two cells on the retinal surface must be capable of communicating regardless of their separation if the simple systems matching mechanism is to produce a globally ordered mapping. Experiments III through VIII were run under this assumption. As stated in the discussion of the BAM, we feel that this assumption is not necessarily true. Instead, the maximum separation allowing effective communication should be reduced to some relatively small value, perhaps the diameter of the receptive field.

We now briefly discuss the Marker Induction model of Willshaw and von der Malsburg as a sophisitcated representative of the point-to-point chemoaffinity approach. The Marker Induction model (Willshaw 1979) involves the specification of the tectal surface by actions of the incoming fibres with the specificity determining, and determined by, the differential growth of synapses between retinal fibres and tectal cells. The retinal surface is posited to possess concentration gradients of a number of transportable substances, with at least one for each spatial dimension. Each retinal cell continually absorbs each of these substances at rates proportional to the concentrations at the cell's location. Thus the cell's retinal location can be uniquely determined by the vector of concentrations. The substances are moved to the synapses by axonal transport where they are injected into the postsynaptic cells at a rate proportional to their concentration and the strength of the synapse.

Each synapse between a retinal fibre and a tectal cell is described by two quantities: strength and fitness. The strength is an indication of

the rate of transfer of the substances between pre- and postsynaptic cells. The fitness describes the similarity between the substance concentration vectors of the pre- and postsynaptic cells. The actual interaction between synapses is governed by a set of three rules:

1. The strength of a synapse is proportional to its fitness. The greater the fitness, i.e. the closer the concentration vectors, the greater the strength.

2. The sum of the strengths of all of the synapses of each presynaptic cell is stipulated to be fixed. This accomplishes two things: first, no synapse can grow without bound; and second, this provides competition between synapses of the same cell. If a particular synapse is to be strengthened, the other synapses must be weekened accordingly.

3. Finally, each axon forms new branches in the neighbourhood of existing ones and branches with synapses whose strengths are below a minimum value are removed.

The above assumptions and rules provide a method for producing locally continuous maps. However, since the model contains no specific orientation information, there is no preference for one particular final organization over another. In computer simulations of the one dimensional version of this model, an initially random organization resulted in piecewise continuous maps with no particular global organization - similar to the results seen in our Experiment II. Willshaw and von der Malsburg provide orientation information by giving the initial map some order. They place the presynaptic fibre terminations in sections of the tectum which approximate the desired final locations.

With this model, Willshaw and von der Malsburg are able to produce mapping behavior consistent with experimental data from both regeneration and developmental experiments.

The Marker Induction Model utilizes information which completely specifies the two cellular layers but uses no interaction information to produce behavior seen in the experimental paradigms. Further, it is clear that the amount of information available to the Arrow Model and BAM is insufficient. The question then arises as to the minimum amount of information which my be employed by a model accounting for all of the experimental data. Further, what mechanisms are used by such a model? It is our opinion that both the system matching and chemoaffinity approaches have their merits. The basic mechanism of the model presented in the next section is a hybridization of these two ideas and is posited to have available information which is more specific than that used by the system matching models yet not as specific as that used by the chemoaffinity models.

VI. XBAM - The Extended Branch-Arrow Model

The Extended Branch-Arrow Model (XBAM) is the successor to the Branch-Arrow Model outlined in section III. It adds a branch-surface interaction mechanism to the neighbourhood and boundary interaction mechanisms of the physical influence component of BAM. This extended version appears to account for an even larger body of experimental data than does BAM.

In the Arrow Model, each fibre would interact with at most one of its eight adjacent sites at each iteration. Switching interaction alone was sufficient to account for much of the experimental evidence but random stepping had to be added to account for the expansion results (Schmidt 1978a, 1978b). Even with this addition, the Arrow Model cannot account for the small class of graft translocation experiments (Hope 1976). In addition, when the distance on the retina allowing an effective exchange of information is reduced from the entire retinal expanse to a fraction of that distance, the global behavior degrades markedly. By contrast, the XBAM model is able to account for essentially all of the significant experimental results.

The XBAM physical infuence component consists of three factors. The first two are exactly the neighbourhood interaction and boundary influences defined in BAM, see Section II. The final factor, $\vec{S}_b$, provides the degree of global information required to account for the translocation experiments. This factor describes the interaction between the branches and the tectal surface. As in BAM, these components are combined with the average influence felt by all of the branches of a fibre to form the total influence felt by each branch during a given iteration, see equation (8).

$$\vec{S}_b = W_s(M(P_r(b),P_t(b))) \; \vec{U}_s(P_r(b),P_t(b)) \qquad (8)$$

where the weight W_S (due to difference of the markers) is described below in equation (9); $P_r(b)$ is an encoding of the retinal position of the soma of the cell emitting branch b; $P_t(b)$ is an encoding of the tectal position of branch b corresponding to the encoding P_r; $M(p,q)$ is a measure of the difference between the retinal and tectal positions; and $\vec{U}_s$ is the unit vector from the branch's current position to its desired final position.

A fibre interacts with the surface of the tectum by way of its branches. Each branch of a fibre is thought to be marked in some manner according to the retinal position of its soma. The marker need not be an indicator of its exact position but rather a marker encoding its general location, e.g. the position should accurate to within plus or minus the distance allowing effective retinal communication. That is, the marker here is to be considered in the sence of a general position indicator as opposed to a point to point chemoafinity. The tectal surface is also posited to be labelled in a similar manner. Each of the branches sample the marker on the tectal surface. The surface influence contains a weight, W_S, which is proportional to the difference between the retinal and tectal labels.

$$W_s(M(a,b)) = \begin{cases} 1 & \text{if } M(a,b) > t_2 \\ \dfrac{M(a,b) - t_1}{t_2 - t_1} & \text{if } t_1 \leqq M(a,b) \leqq t_2 \\ 0 & \text{otherwise} \end{cases} \qquad (9)$$

where t1 and t2 are thresholds which determin the interval on the retina allowing effective communication.

The average of the influences, $\vec{A}_b$, felt by the branches of a particular fibre is given by equation (10)

$$\vec{A}_b = \frac{1}{m} \sum_{k \in F_b} (a_7 \vec{I}_k + a_8 \vec{E}_k + a_9 \vec{S}_k) \qquad (10)$$

where the sumation ranges over the set F_b of all branches k from the same retinal fibre as b, m is the number of branches in F_b, and a_7, a_8, and a_9 are weighting constants.

The updating processes used in the Extended Branch-Arrow Model consists of four components. For each of the branches, the interaction influence, boundary influence, surface influence, and the average influence components are combined in a weighted average to form the movement of the branch.

$$\vec{M}_b = a_{10}\vec{I}_b + a_{11}\vec{E}_b + a_{12}\vec{S}_b + a_{13}\vec{A}_b \qquad (11)$$

where a_{10}, a_{11}, a_{12}, and $a_{13}$are weighting constants.

The following section provides the simulation behavior of this hybrid model.

VII. Computer Simulation of XBAM

This section contains simulation results of the Extended Branch-Arrow Model (XBAM). Experiments IX through XVI utilize the same experimental paradigms as Experiments I through VIII, respectively. In each case, the reader is refered to the appropriate experiment in Section III for a discussion of the relevant physiological data. The final experiment, XVI, investigates the simulation behavior under a developmental paradigm.

Experiment IX.

In this experiment, the development of the projection from a normal retina onto a normal tectum was studied. Figure VII.1 illustrates the initial random positioning of the branches. Figure VII.2 contains the state of the mapping after 10000 iterations of XBAM. As in Experiment I, retinal cells were allowed to eschange information regardless of the distance between them. As expected from Experiment I with BAM, XBAM produced an ordered mapping.

Figure VII.1, VII.2

Experiment X.

This experiment tests the effect of reducing the distance allowing effective communication on the retina, cf. Experiment II. Figure VII.3 contains the mapping after 28000 iterations of XBAM with the retinal distance reduced to roughly one half of the retina. XBAM produced a globally ordered map while BAM produced several superpositioned maps, cf. Figures VII.3 and III.3b. The surface interaction term added enough information to allow the neighbourhood and boundary mechanisms to produce a completely organized projection.

Figure VII.3

Experiment XI.

This experiment involved the same experimental paradigm as Experiment III in Section III in that the caudal half of the tectum was ablated. The key features to note here are the facts that the entire visual field is represented along the dimension where only half of the original surface remains and that along the other dimension, all of the space is utilized.

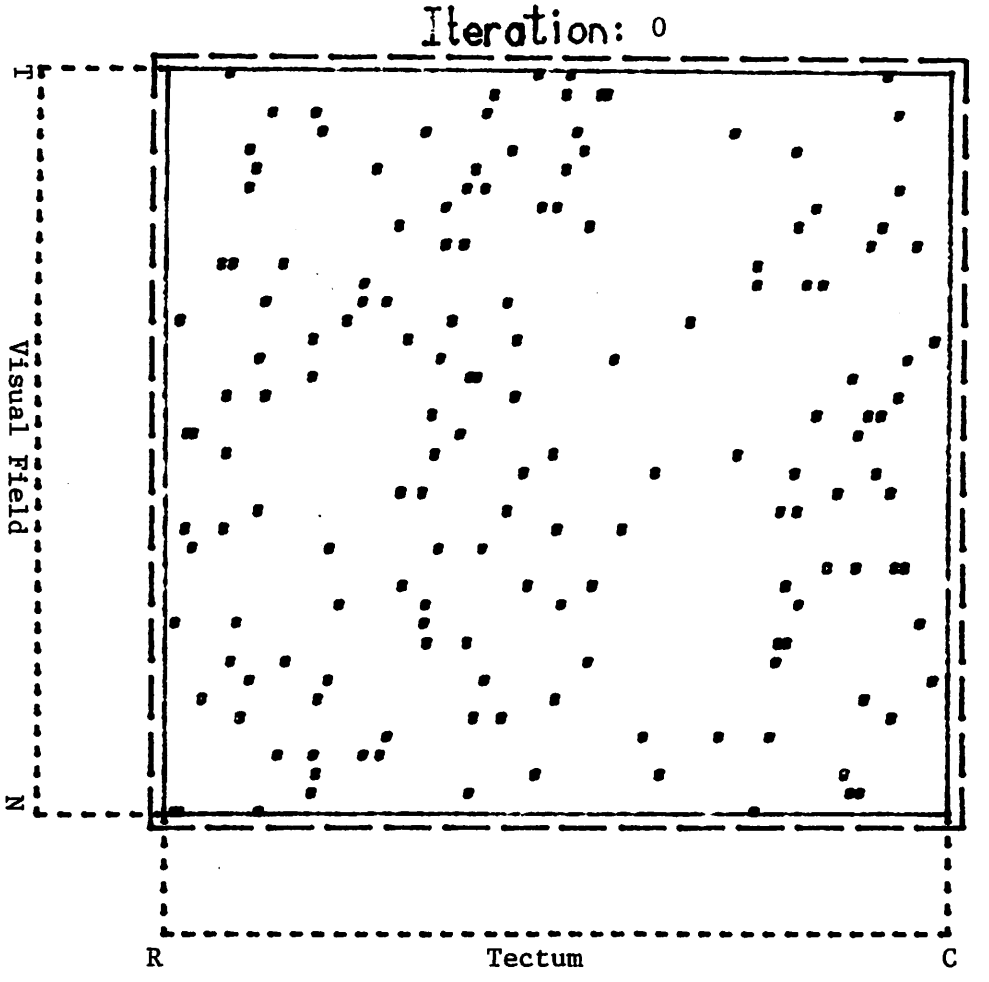

Figure VII.1 Initial branch distribution for the XBAM simulations.
40 fibres with 4 branches/fibre.

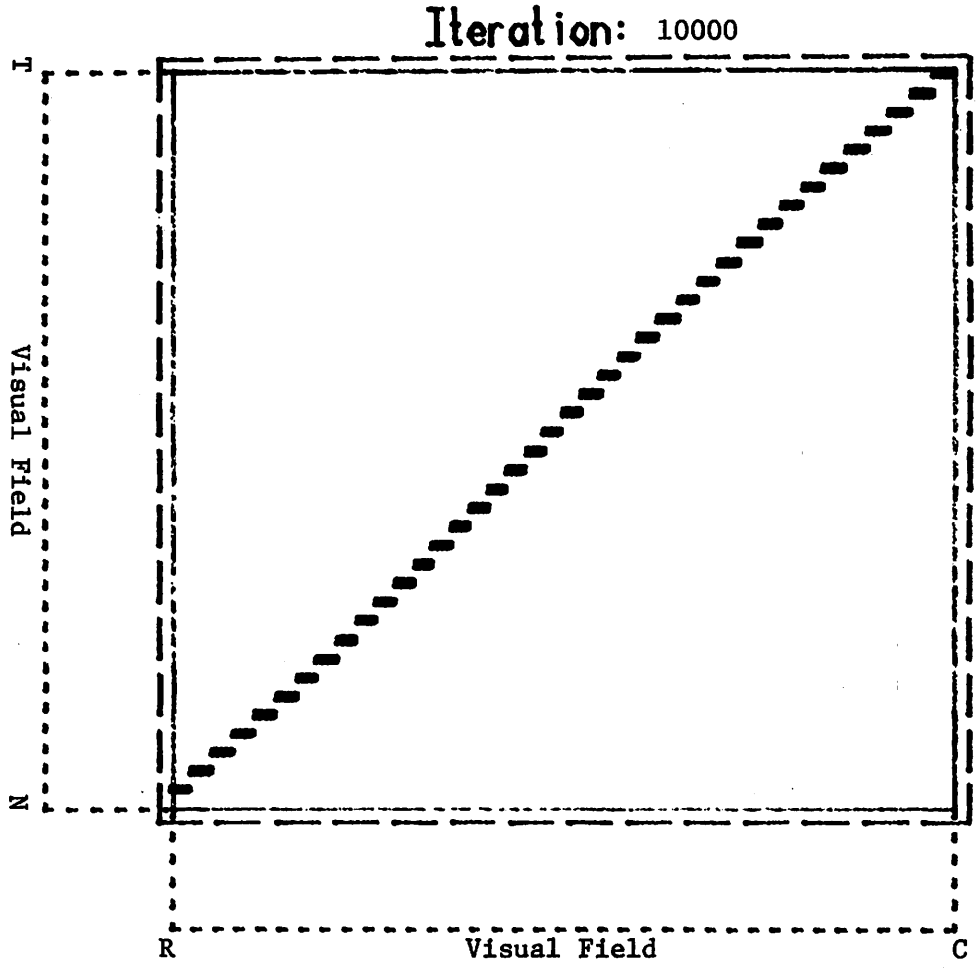

Figure VII.2 Mapping organization after 10000 iterations of XBAM with the retinal distance allowing effective communication equal to the entire retina width.

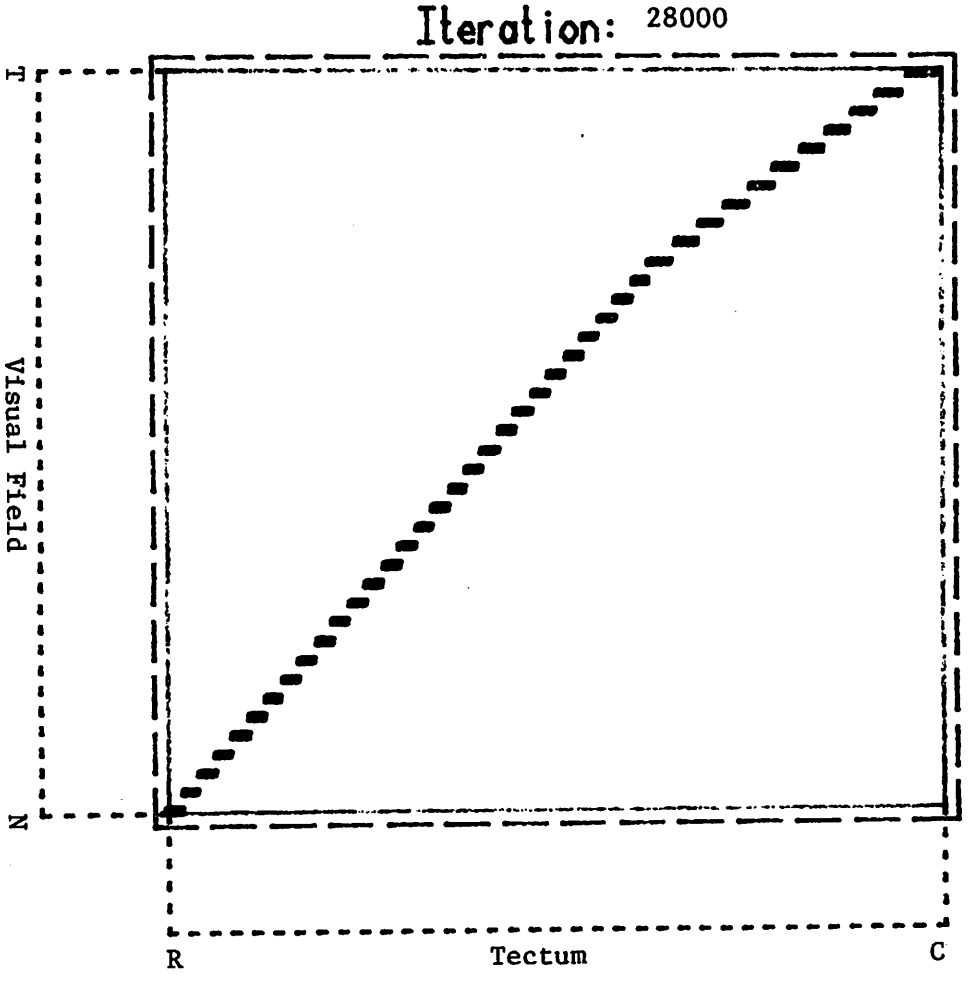

Figure VII.3 Projection after 28000 iterations of XBAM with the retinal interaction distance reduced to roughly 1/2 of the retina width.

Figure VII.4 contains the results from the XBAM computer simulation. The initial termination locations were randomly distributed over the tectal surface. The surface was reduced to one half of its original size. The organization of the projection after 500 iterations of XBAM is shown in the figure. This map shows excellent global organization. The branches in the extreme lower left portion of the field have been forced off of the tectal surface. The magnitude of the effect is determined in part by the relative values of the weighting contants in equations (10) and (11).

Figure VII.4

Experiment XII.

In this case we are simulating the mapping resulting between a hemiretina and an intact tectum (Schmidt 1978a). The projection of the half of the visual field represented on the remaining hemiretina expands in an orderly manner to completely fill the available space on the tectum. The XBAM simulation results for this situation are given in Figure VII.5. The initial locations for the branches were randomly assigned. The state after 10000 iterations shows complete organization with half of the normal number of fibres mapping onto the complete tectal surface. The mapping does not fill the entire rostral section of the tectum. This is due to a slight imbalance in the weighting constant values.

Figure VII.5

Experiment XIII.

A direct extension to the hemiretina, full tectum experiments involves studying the projection resulting when hemiretinae from different eyes are fused to form a single eye.

Figure (VII.6,VII.7) contains the results from computer simulations of the XBAM when a double nasal eye maps onto the tectum. Figure VII.6 results from hemiretinae with their orientations retained so that the maps are oriented the same. Figure VII.7 was produced with the orientation of one half of the retina reversed.

Figure VII.6, VII.7

Notice that in both cases the global organization of the field represented on each hemiretinae is maintained. However, the projection has expanded to cover most of the available tectal surface.

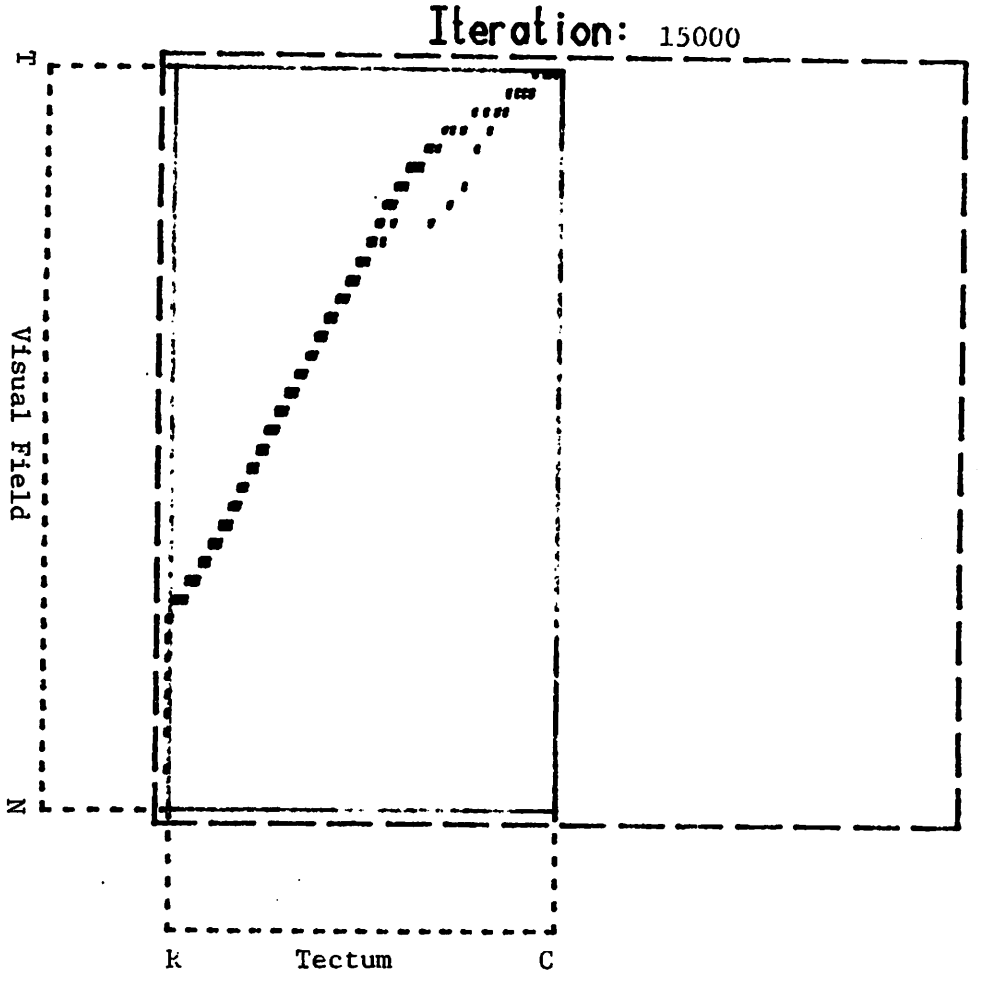

Figure VII.4 XBAM simulation results of a full retina mapping onto a half tectum. 15000 iterations.

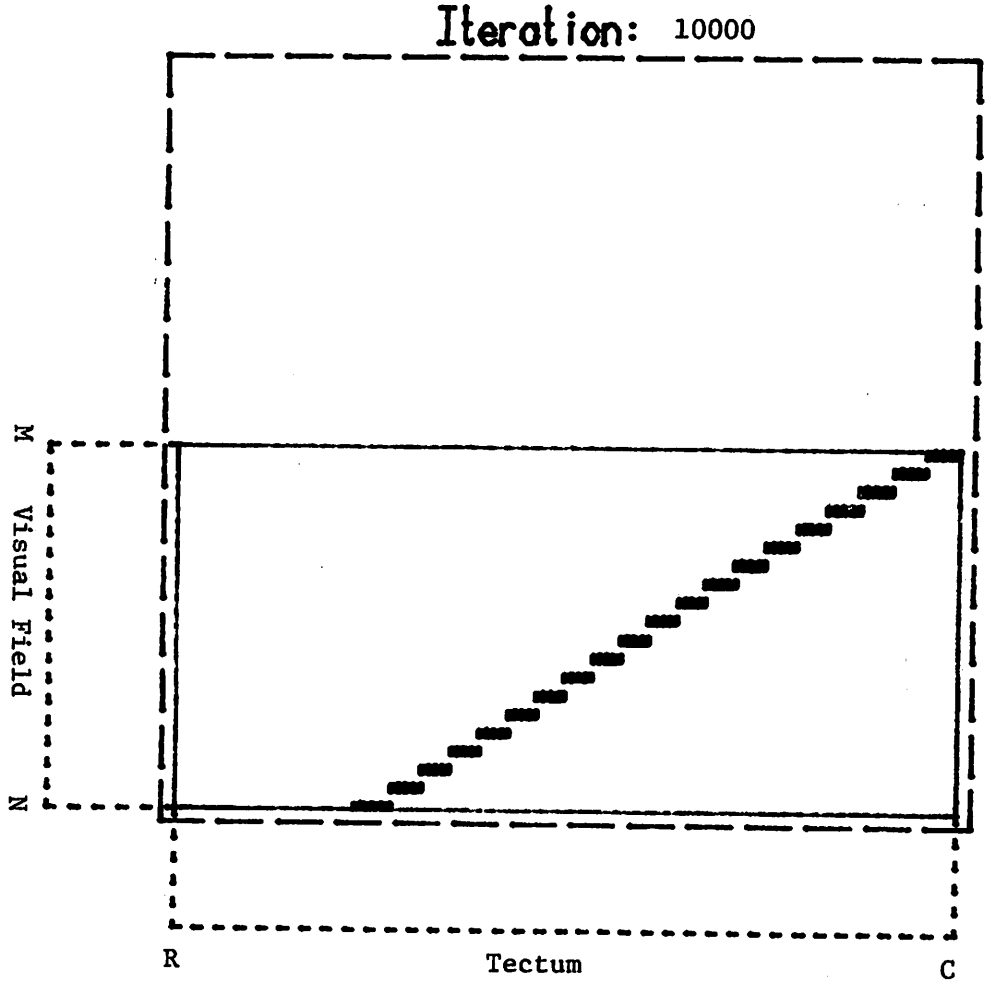

Figure VII.5 XBAM simulation results of a hemiretina projecting onto a full tectum, 10000 iterations.

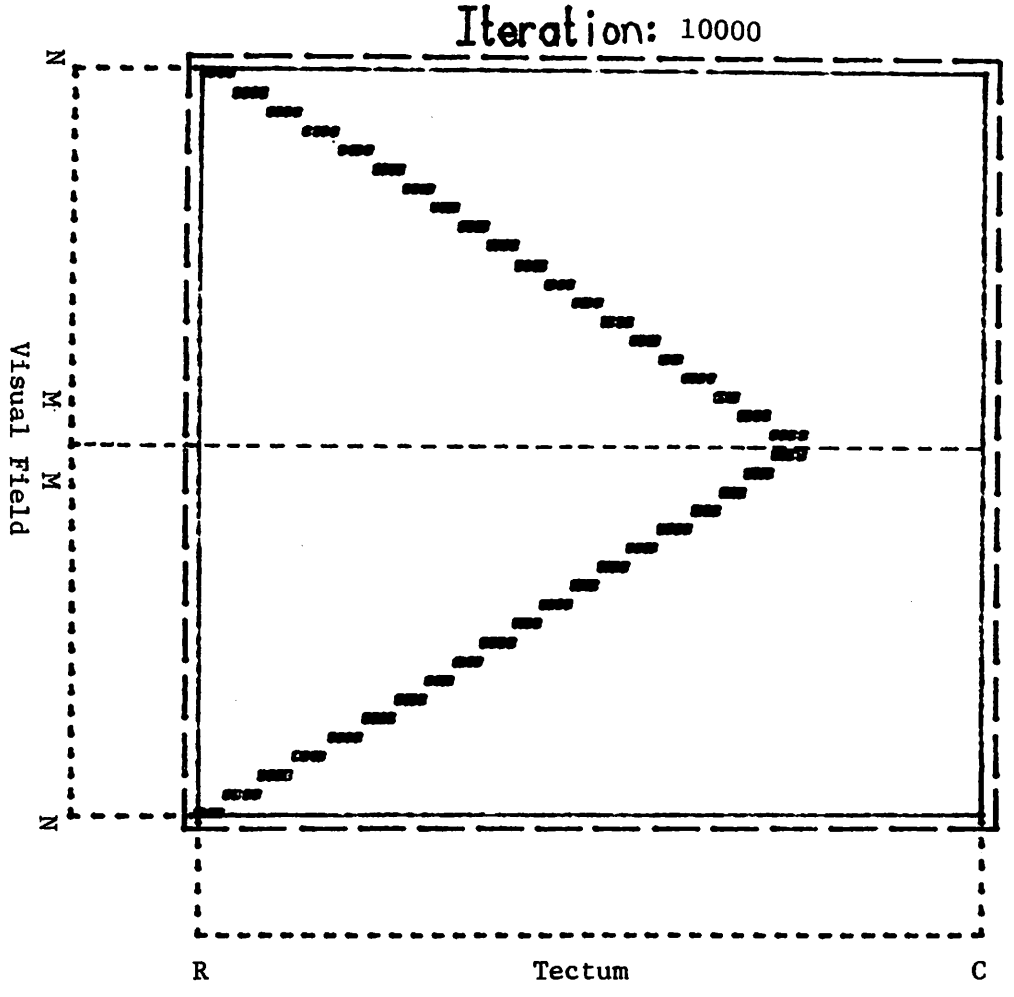

Figure VII.6 XBAM results of double-nasal compound eye experiment. 10000 iterations.

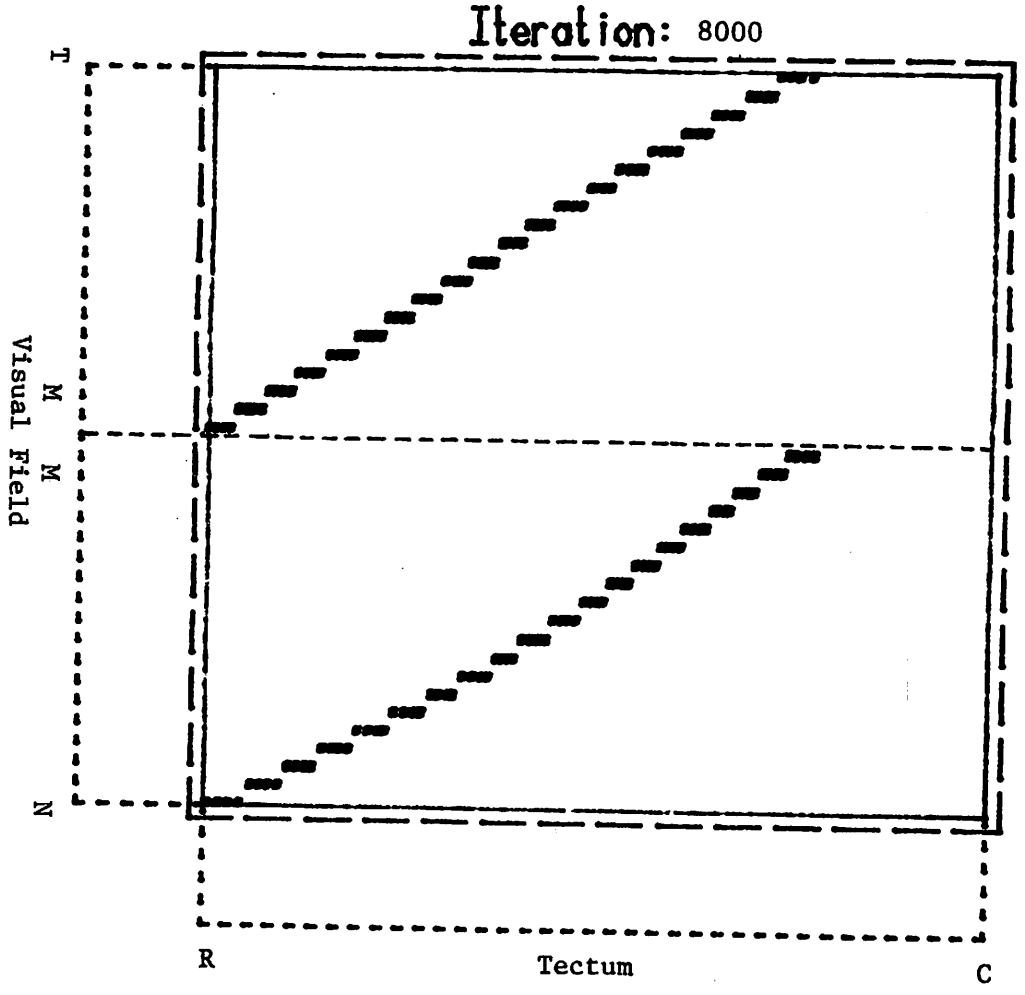

Figure IV.7 Results of XBAM simulation of nasal-temporal compound eye experiment. 8000 iterations.

Experiment XIV.

The simulation of the XBAM is one dimensional as was BAM and the 90 degree rotation experiments cannot be performed and the two forms of the 180 degree rotations are equivalent. Figure VII.8 illustrates the state of organization of the branch termination locations after 8000 iterations. The initial configuration was again random.

Figure VII.8a

Notice that the most caudal section of the tectum receives information only from the temporal area in the visual field. The projection in that area is reasonably well ordered. The fibres from the nasal section of the visual field are moving toward the rostral section of the tectum. The fibres which should project onto the grafted area are trapped between those in the rostral one third of the tectum and those moving toward that end. The organization in the rostral one third of the tectum is also reasonably well ordered.

Experiment XV.

Experiments VI and VII illustrated that the simple BAM cannot produce behavior exactly as that found in graft rotation experiments. This experiment involves simulating XBAM under the same conditions as described in Experiment III in which the positions but not the orientations of two grafts are altered.

Simulation results from the translocated graft experiment appear in Figure VII.8b. Perfect organization in the one dimensional case would appear as line segments l_1 through l_5. Recall that BAM produced a completely normal mapping, cf. Figure IV.15. XBAM produces behavior closer to that observed experimentally. The disorder in the map is the result of conflicting information from the surface and neighbour interactions. Behavior more closely resembling the ideal case could be produced by appropriately adjusting the weighting constants in equations (10) and (11).

Figure VII.8b

Experiment XVI

This experiment is designed to compare the behavior of the XBAM simulation with the physiological results obtained during development in a

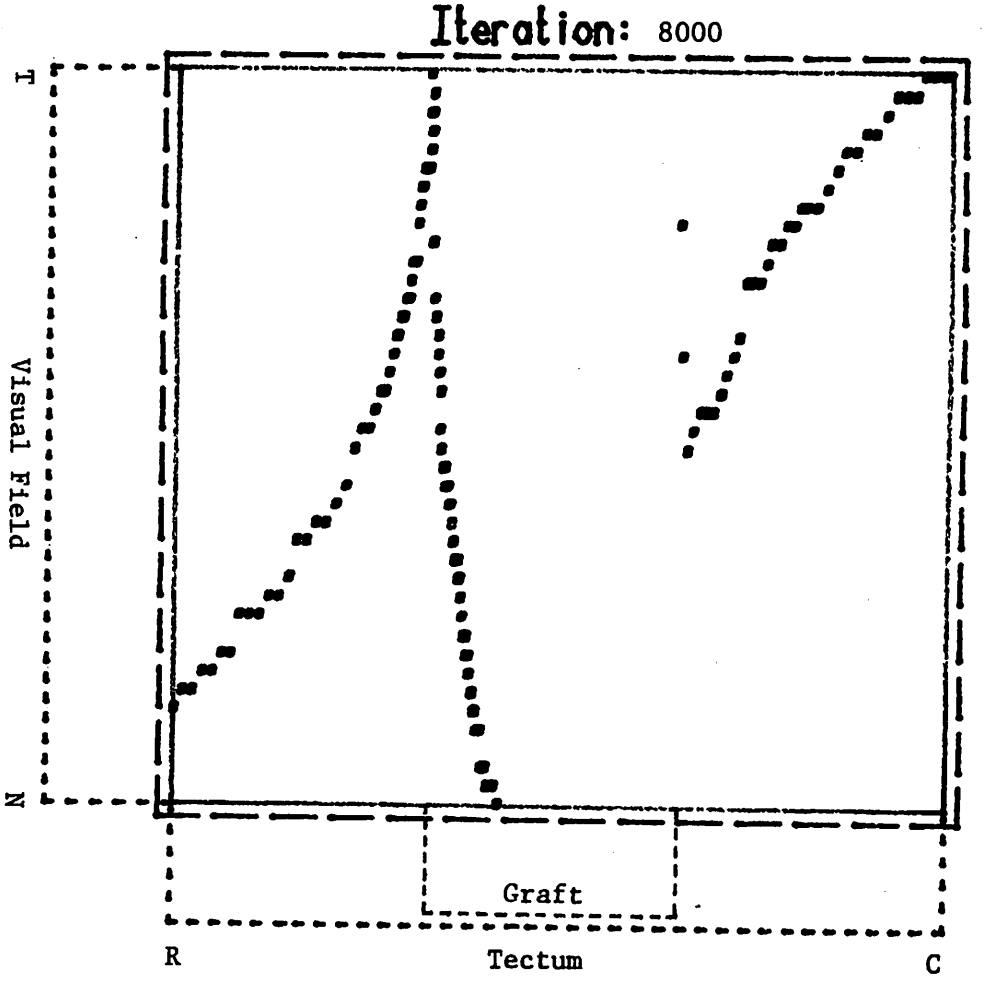

Figure IV.8a XBAM simulation results of full retina projecting onto a tectum with one graft excised and inverted.

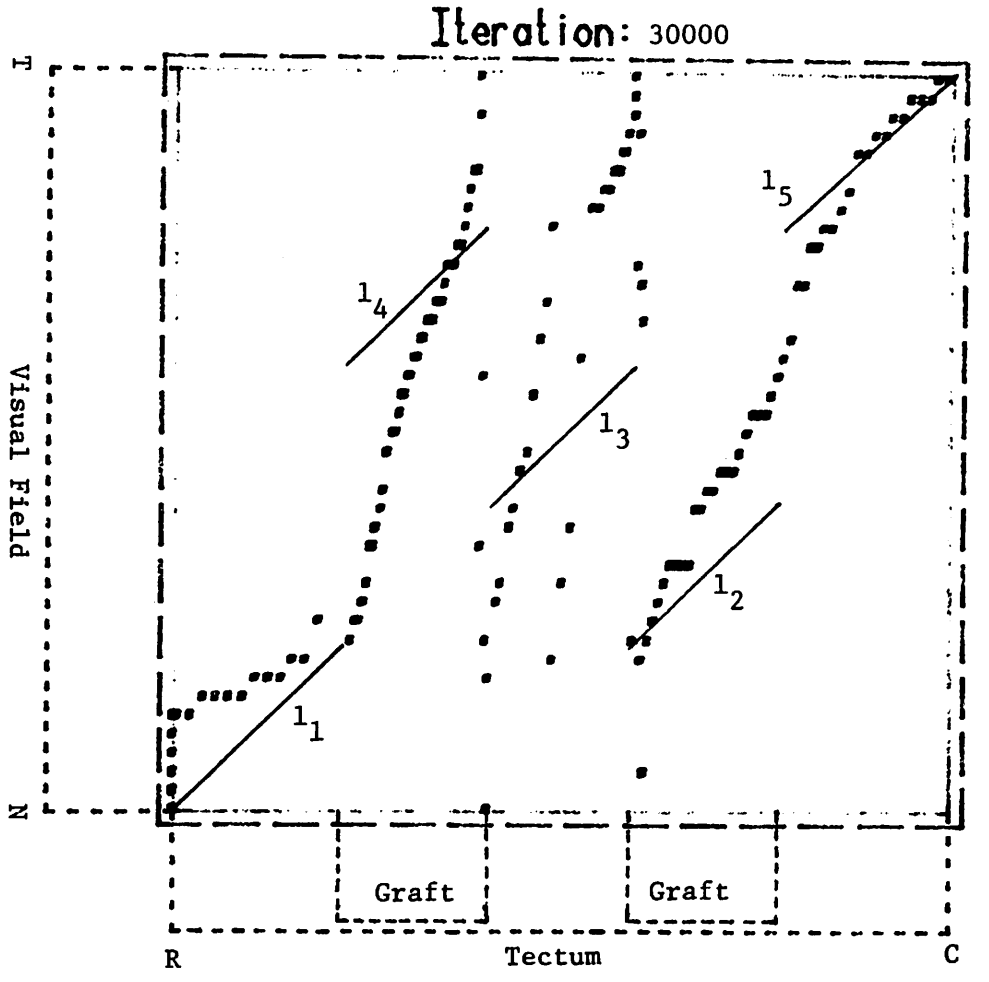

Figure VII.8b XBAM results of a full retina mapping onto a tectum with two grafts translocated.

more realistic paradigm than its counterpart in Section III, Experiment VIII. The retinal and tectal cell sheets grow at different rates and with different geometries. The retina tends to develop from the center outward in all directions at a uniform rate. The first section of the tectum to develop is the rostrocaudal section. Growth occurs primarily in the caudal and lateral direction. Figure VII.9 illustrates physiological results produced by Gaze (1974).

Figure VII.9

The figure contains mappings of the projection of the visual field at various larval stages. There are two interesting features in the data. First, the projection is ordered and initially covers only part of the tectal surface. As the organism continues to develop, the projection expands to fill the entire tectal surface. Second, the projection of the temporal visual field is quite large in comparison to to those of the medial and nasal field. Only after all of the tectal space has been filled does the projection begin to adjust to its normal proportions.

Figure VII.10 contains the XBAM simulation results. In this case, the retina is "grown" from the center outwards. The branches of two fibers are added every 200 iterations. In all cases, the branches of the new fibers are randomly distributed over the tectal surface as delimited in Figure VII.10a. During the same iteration,, the tectal surface is increased in size. The rate of growth in the caudal direction is three times that in the rostral direction. Notice that the middle of the projection onto the tectum is organized as early as iteration 600, cf. Figure VII.10b, with only 8 fibers represented. As fibers are added from the edges of the retina, the projection remains organized. The tight packing and steep angle seen in the center of the projection indicates that the projection of the medial section of the visual field is compressed as seen in the physiological data. A distinctive "S" shape is evident in the mapping after iteration 2400, Figure VII.10e. The tails of the projection curve since they cover proportionally more of the tectal surface than does the center. In figure VII.10g the branches of the fibres near the center of the projection are tightly packed while the branches of the fibers near the ends are spead out. It should also be noted that the projection is slowly moving in a caudal direction. Continued iteration of the simulation would result in a shift of the mapping in the caudal direction until a mapping projection uniformly covers the entire tectal surface as in Figure P.2.

Figure VII.10a-g

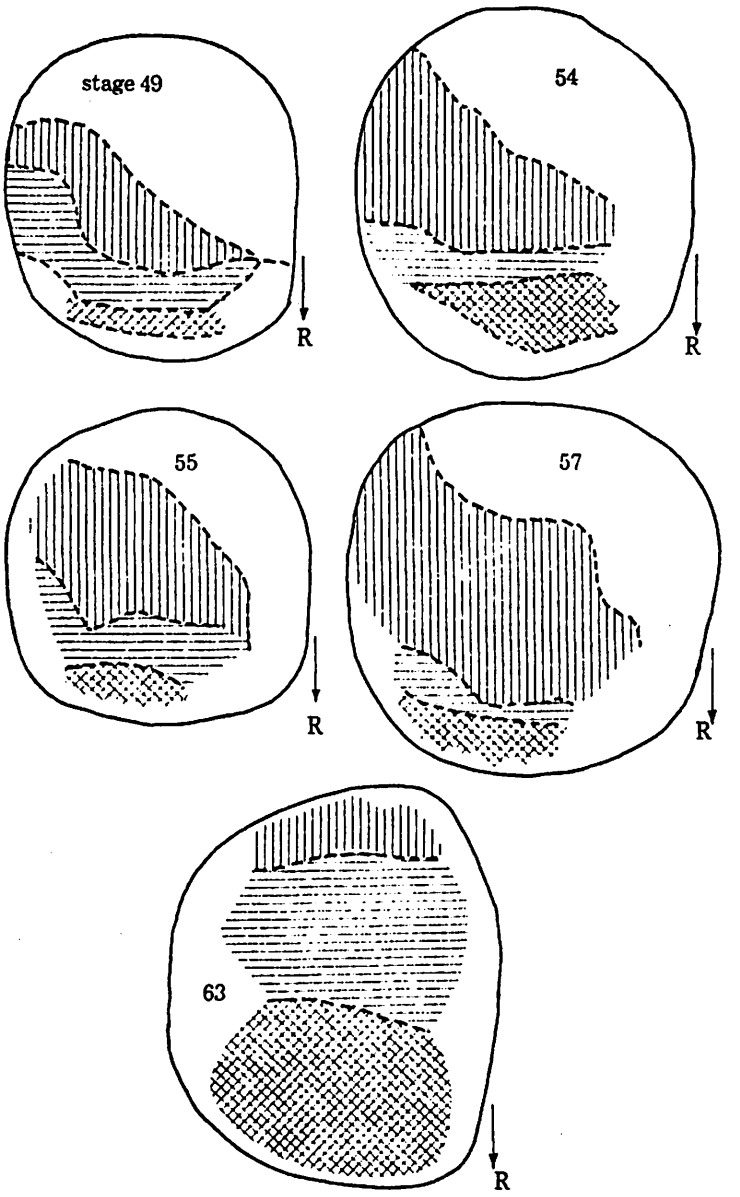

Figure VII.9 Physiological data of visual field projection mapping during various larval stages (Gaze 1974).

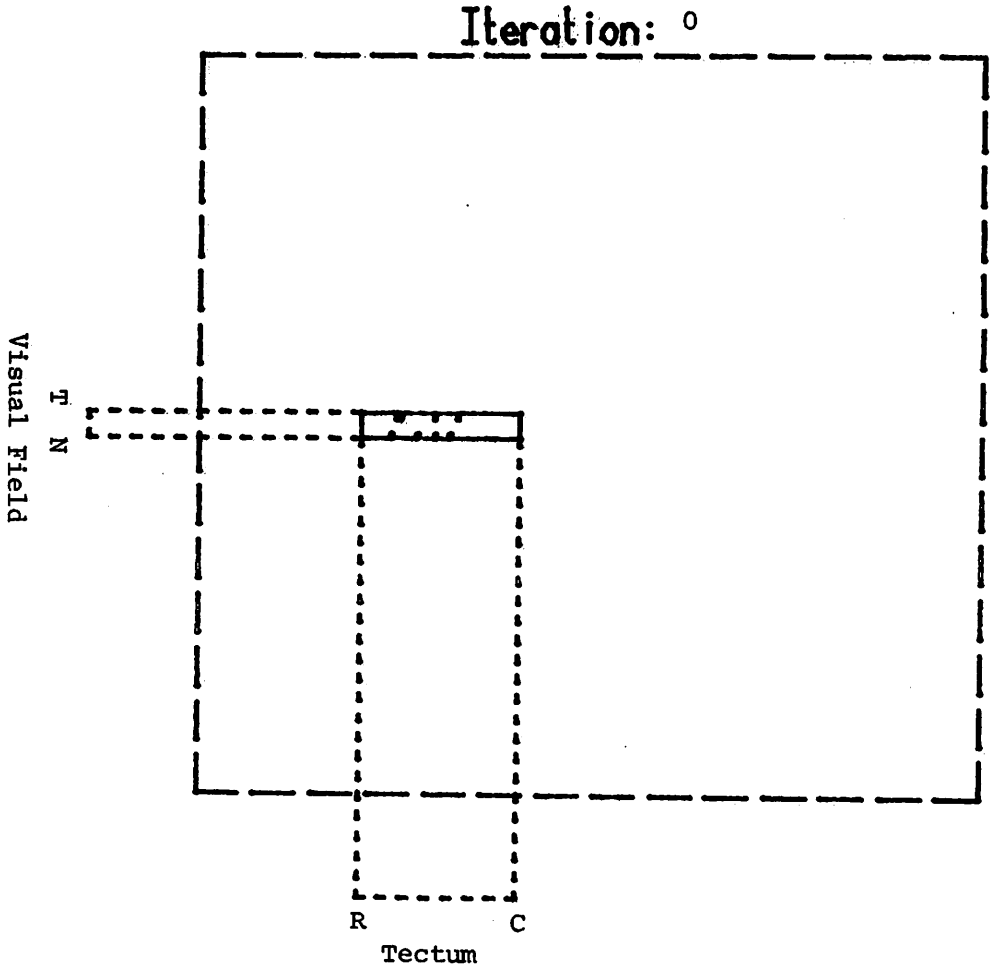

Figure VII.10a

Figure VII.10a-g XBAM simulation of developping visual field and tectum. The visual field grows uniformly out from the center while the tectum grows three times as fast in the caudal direction as in the rostral direction. a) initial state, b) 600 iterations, c) 1200 iterations, d) 1800 iterations, e) 2400 iterations, f) 3000 iterations, g) 3800 iterations.

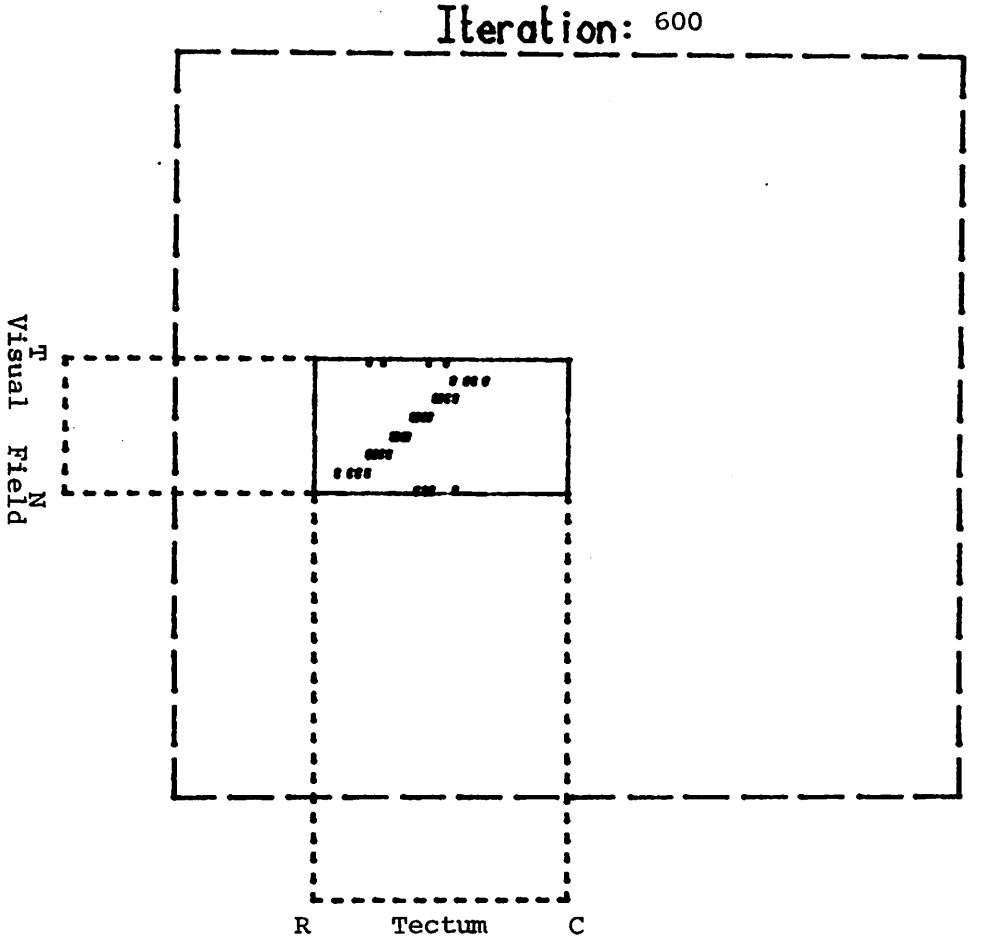

VII.10b

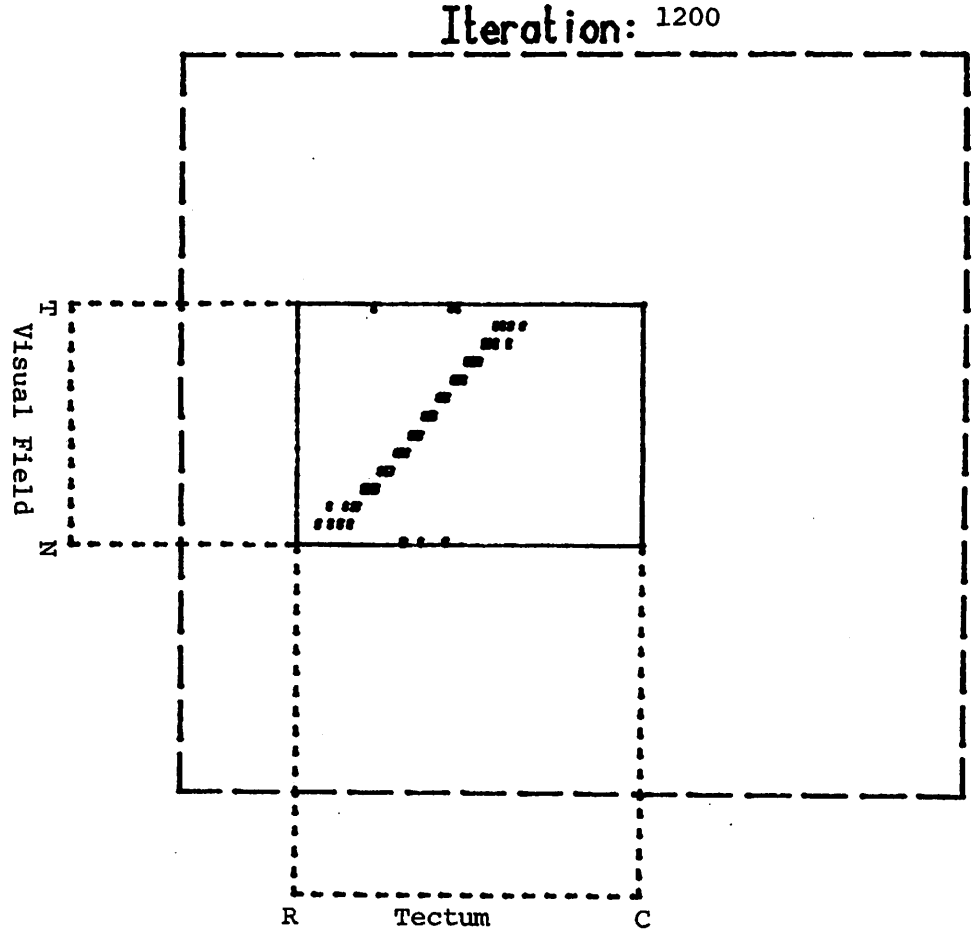

VII.10c

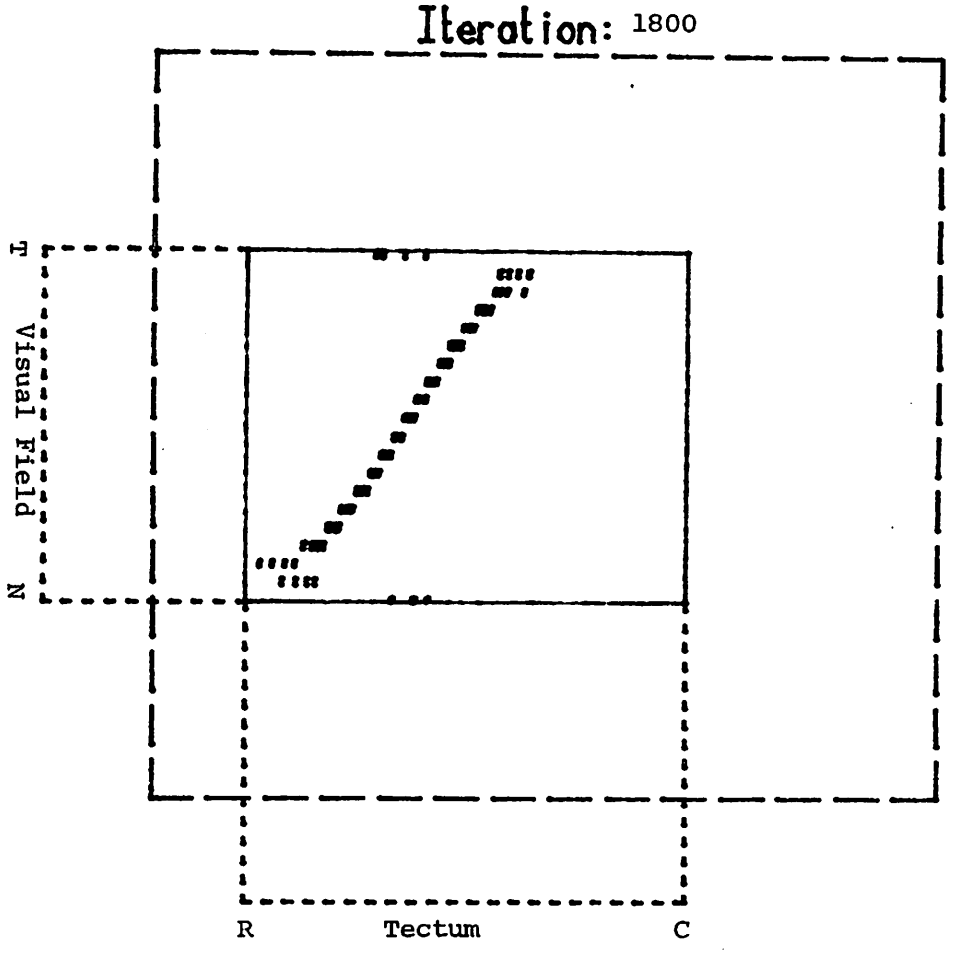

VII.10d

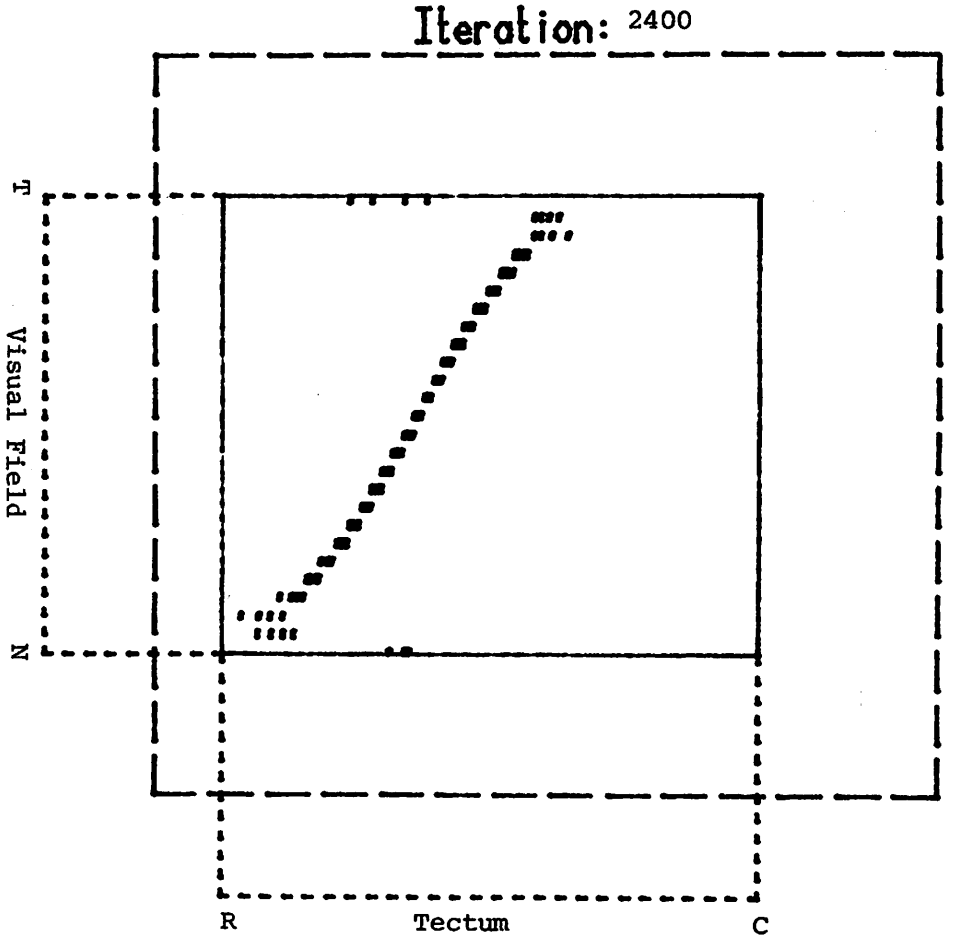

VII.10e

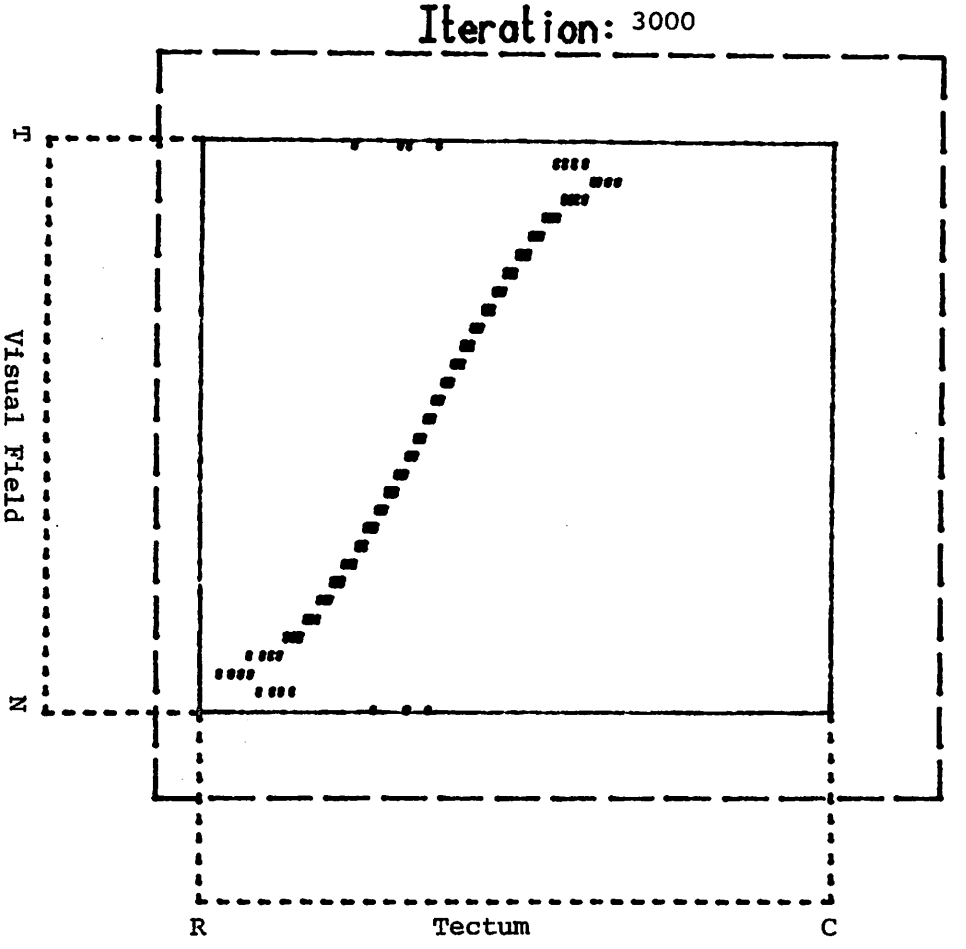

VII.10f

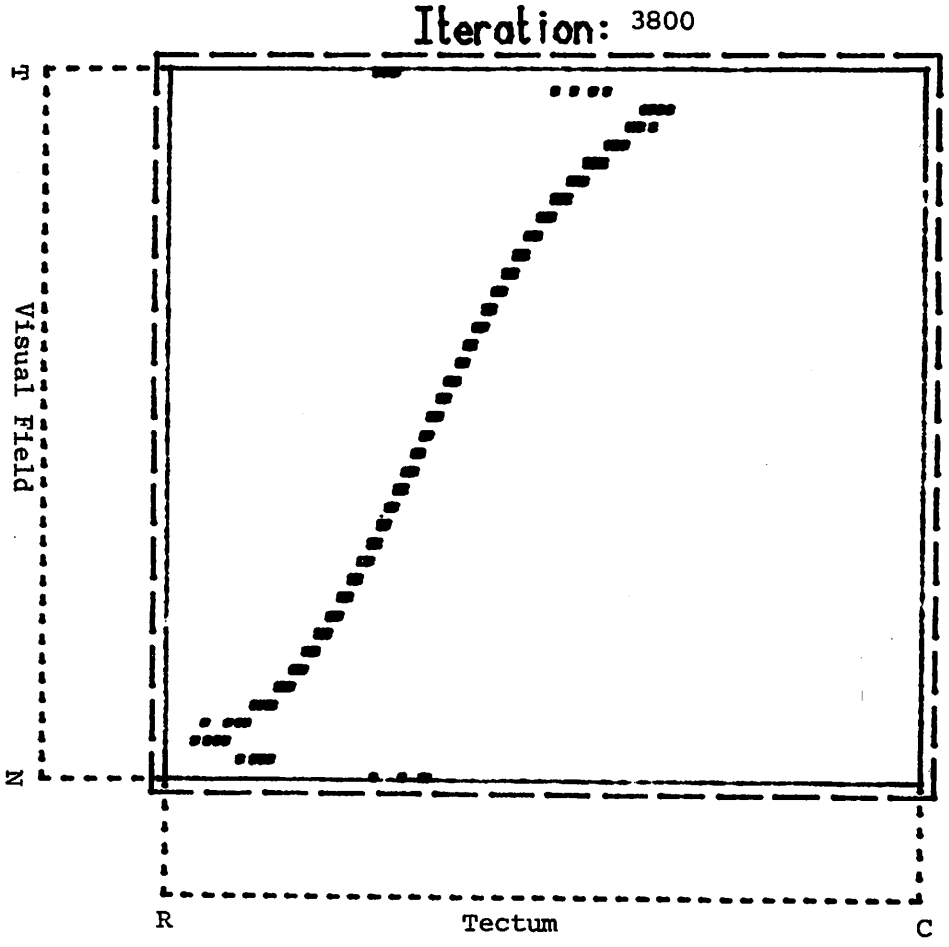

VII.10g

VIII. Conclusion

The systems matching theory of the process by which the retinotectal mapping is produced in lower vertebrates has been discussed. In this light, we presented the Branch-Arrow Model, BAM, as an extension to the Arrow Model of Hope et al. This model is continuous in nature and includes a generalized neighbourhood interaction mechanism as well as explicit boundary interaction. Its behavior was demonstrated through the use of computer simulations. These experiments demonstrated that the systems matching approach utilizing effective communication between any two retinal cells can account for the majority of the physiological experimental results. However, if the retinal distance allowing communication is reduced to a fraction of the total retinal expanse, the behavior degrades considerably. This leads to the conclusion that neighbourhood interaction mechanisms alone lack sufficient information to produce global organization.

The chemoafinity theory as delineated by the Marker Induction Model of Willshaw and von der Malsburg was then discussed. This elegant model can produce behavior similar to the experimental results but requirès a degree of initial organization in order to produce a final map which is globally continuous. While this requirement may not be unreasonable, the more general question of the amount of information, or specificity, required by a model to explain the physiological results remains. The Extended Branch-Arrow Model, XBAM, was presented as a compromise between these two approaches.

This model combines the local systems matching mechanisms apparent in BAM with a component describing a rough, inaccurate global positioning mechanism derived from the chemoaffinity theory. The behavior of this hybrid model was investigated through computer simulation and was shown to be in good agreement with the physiological data. The authors propose XBAM not as a competitor to the systems matching and chemoaffinity models but as an example of a blend of certain interesting features of the two approaches.

Bibliography

Cook, J.E. & Horder, T.J. 1974 Interactions between optic fibers in their regeneration to specitic sites in the goldfish tectum. J. Physiol. 241, 89-90P.

Feldman, J.D., Keating, M.J., & Gaze, R.M. 1975 Retino-tectal mismatch: a serendipitous experimental result. Nature, Lond., 253, 445-446.

Gaze, R.M., Jacobson, M., & Szekely, G. 1963 The retino-tectal projection in Xenopus with compound eyes. J. Physiol., 165, 484-499.

Gaze, R.M., Jacobson, M., & Szeleky, G. 1965 On the formation of connections by compound eyes in Xenopus. J. Physiol., 176, 409-417.

Gaze, R.M. & Sharma, S.C. 1970 Axial differences in the reinnervation of the goldfish optic tectum by regenerating optic fibers. Expl. Brain Res. 10, 171-181.

Gaze, R.M. & Keating, M.J. 1972 The visual system and "neuronal specificity". Nature 237, 375-378.

Gaze, R.M., Keating, M.J., & Chung, S.H. 1974 The evolution of the retinaotectal map during development in Xenopus. Proc. R.Soc. Lond. 185, 301-330.

Hope, R.A., Hammond, B.J., & Gaze, F.R.S. 1976 The arrow model: retinotectal specificity and map formation in the goldfish visual system. Proc. R. Soc. Lond. 194, 447-466.

Horder, T.J. 1971 Retention by fish optic nerve fibres regenerating to new terminal sites on the tectum, "chemospecific" affinity for their original sites. J. Physiol. Lond. 216, 53-55.

Horder, T.J. & Martin, K.A.C. 1977 Translocation of optic fibers in the tectum map be determined by their stability relative to surrounding fiber terminals. J. Physiol., Lond., 271, 23-24P.

Humphery, M.F. and Beazley, L.D. 1981 An electrophysiological study of early patterns of the retinotectal projection during optic nerve regeneration in Hyla Moorei. submitted to Brain Research.

Hunt, R.K. & Jacobson, M. 1973 Development of neuronal locus specificity in Xenopus retinal ganglion cells after surgical transection or after fusion of whole eyes. Dev. Biol., 40, 1-15.

Jacobson, M. & Gaze, R.M. 1965 Selection of appropriate tectal connections by regenerating optic nerve fibers in adult goldfish. Exp. Neurol., 13, 418-430.

Levine, R. & Jacobson, M. 1974 Development of optic nerve fibres is determined by positional markers in the frog tectum. Exp. Neurol. 43, 527-538.

Maturana, H.R., Lettvin, J.Y., McCulloch, W.S., & Pitts, W.H. 1959 Evidence that the cut optic nerve fibers in a frog regenerate to their proper places in the tectum. Science, 130, 1709-1710.

Schmidt, J.T. 1978 Expansion of the half retinal projection to the tectum of in goldfish: an electrophysiological and anatomical study. J. comp. Neurol. 177, 257-278.

Schmidt, J.T. 1978 Retinal fibers alter tectal positional markers during the expansion of the half retinal projection in goldfish. J. comp. Neurol. 177, 279-300.

Schmidt, J.T. & Easter, S.S. 1978 Independant biaxial reorganization of the retinotectal projection: a reassessment. Exp. Brain Res. 31, 155-162.

Sharma, S.C. 1972 Redistribution of visual projections in altered optic tecta of adult goldfish. Proc. Nat. Acad. Sci. U.S.A. 69, 2637-2639.

Sharma, S.C. & Romeskie, M. 1977 Immediate 'compression'of the retinal projection to a tectum devoid of degenerating debris, Brain Res. 134, 367-370.

Sperry, R.W. 1943 Visuomotor coordination in the newt (Triturus viridescens) after regeneration of the optic nerve. J. Comp. Neurol., 79, 33-55.

Sperry, R.W. 1944 Optic nerve regeneration with return of vision in Anurans. J. Neurophysiol. 7, 57-70.

Sperry, R.W. 1945 Restoration of vision after crossing of optic nerves and after contralateral transplantaion of eye. J. Neurophysiol. 8, 15-28.

Sperry, R.M. 1963 Chemoaffinity in the orderly growth of nerve patterns and connections. Proc. natn. Acad. Sci., U.S.A. 50, 701-709.

Willshaw, D.J. & von der Malsburg, C. 1979 A marker induction mechanism for the establishment of Ordered neural mappings: its application to the retinotectal problem. Phil. Trans. Proc. R. Soc. Lond. B, 287, 203-243.

Udin, S.B. 1977 Rearrangements of the retinotectal projection in Rana Pipiens after unilateral caudal half-tectum ablation. J. comp. Neurol. 173, 561-582.

Yoon, M.G. 1973 Retention of the original toopgraphic polarity by the 180 degree rotated tectal reimplant in young goldfish. J. Physiol. 233, 575-588.

Yoon, M.G. 1975 Readjustment of retinotectal projection following reimplantation of a rotated or inverted tectal tissue in adult goldfish. J. Physiol. 252, 137-158.

Yoon, M.G. 1976 Progress of topographic regulation of the visual projection in the halved optic tectum of adult goldfish. J. Physiol. 257, 621-643.